SYNTHESIS AND CHARACTERIZATION OF PANI/ZnO BASED ELECTROCHEMICAL SENSOR FOR THE DETECTION OF SOME TOXIC HEAVY METAL IONS

MSc THESIS

ABATE ADEMMA ABUKO

JUNE 2017
HARAMAYA UNIVERSITY, HARAMAYA

Synthesis and Characterization of PANI/ZnO Based Electrochemical Sensor for the Detection of Some Toxic Heavy Metal Ions

A Thesis Submitted to the Department of Chemistry
Postgraduate Program Directorate
HARAMAYA UNIVERSITY

In Partial Fulfillment of the Requirements for the Degree of
MASTER OF SCIENCE IN CHEMISTRY

(PHYSICAL CHEMISTRY)

Abate Ademma Abuko

June 2017
Haramaya University, Haramaya

HARAMAYA UNIVERSITY
POSTGRADUATE PROGRAM DIRECTORATE

As Thesis Research advisors, we hereby certify that we have read and evaluated this thesis work prepared under our guidance, by **Abate Ademma Abuko**, entitled: **"*Synthesis and Characterization of PANI/ZnO Based Electrochemical Sensor for the Detection of Some Toxic Heavy Metal Ions.*"** We recommend that it be submitted as fulfilling the Thesis requirement.

.

Abebaw Adgo (PhD)	_____	_____
Major Advisor	Signature	Date
Tesfahun Kebede (PhD)	_____	_____
Co-Advisor	Signature	Date

As member of the board of examiners of the MSc Thesis Open Defense Examination, I certify that I have read and evaluated the MSc Thesis Research prepared by **Abate Ademma** and examined the candidate. I recommend that the Thesis be accepted as fulfilling the MSc Thesis research requirement for the Degree of **Master of Science in Chemistry (Physical)**.

_____	_____	_____
Chairperson	Signature	Date
_____	_____	_____
Internal Examiner	Signature	Date
_____	_____	_____
External Examiner	Signature	Date

DEDICATION

I dedicate this MSc Thesis work to my lovely mother, **W/ro Laillo Jalammo**.

STATEMENT OF THE AUTHOR

By my signature below, I declare and affirm that this Thesis is my own work. I have followed all ethical and technical principles of scholarship in the preparation, data collection, data analysis and compilation of this Thesis. Any Scholarity matter that is included in the Thesis has been given recognition through citation.

This Thesis is submitted in partial fulfillment of the requirements for an MSc degree at the Haramaya University and is made available to borrowers under the rules of the Library. I solemnly declare that this Research Thesis has not been submitted to any other institution anywhere for the award of any academic degree, diploma or certificate.

Brief quotations from this Research Thesis may be made without special permission provided that accurate and complete acknowledgment of the source is made. Requests for permission for extended quotation from or reproduction of this Thesis in whole or part may be granted by the Head of the Department when in this or her judgment the proposed use of material is in the interest of scholarship. In all other instances, however, permission must be obtained from the author of the Thesis.

Name: Abate Ademma Signature: _____

Date of submission: 22-Jun-2017

Department: Chemistry

ACRONYMS AND ABBREVIATIONS

AAS	Atomic Absorption Spectroscopy
APS	ammonium persulfate
CPs	Conducting polymers
CV	Cyclic Voltammetry
DMF	N,N-dimethyl Formamide
E_{pa}	Anodic Peak Potential
E_{pc}	Cathodic Peak Potential
FTIR	Fourier Transforms Infrared
GCE	Glassy Carbon Electrode
i_{pa}	Anodic Peak Current
i_{pc}	Cathodic Peak Current
mV	Milivolts
OSW-ASV	Ostroyoung Square Wave-Anodic Stripping Voltammetry
PANI	Polyaniline
pH	Power of Hydrogen
PPb	Parts Per Billion
PPm	Parts Per Million
R^2	Linear Regression
HRSEM	High Resolution Scan Electron Microscopy
HRTEM	High Resolution Transmission Electron Microscopy
THM	Toxic Heavy Metals
v	Scan rate
WHO	World Health Organization
μA	Microampere

BIOGRAPHICAL SKETCH OF THE AUTHOR

The author was born from his father Ademma Abuko and his mother Laillo Jallamo on December 4, 1988 in Eastern Badawacho Woreda, Haddiya Zone, Southern Nation Nationality and Peoples Regional State, Ethiopia. He first started his primary education in Tikare Anibassa Elementary School. He attended his secondary school in Shone Secondary and Preparatory School. After completing secondary school, he joined Mizan-Tepi University, College of Natural and Computational Sciences, Department of Chemistry in 2007/08 and graduated with B.Ed degree in Chemistry in 2011. Soon after graduation, he was employed by MOE to work under SNNPR Education Bureau, in Hadiya Zone. After four years service, he joined Haramaya University, College of Natural and Computational Sciences, Department of Chemistry in 2015/16 to pursue his postgraduate studies in Chemistry (Physical Chemistry), under the Regular Postgraduate program.

ACKNOWLEDGEMENTS

I would like to thank my advisor Dr. Abebaw Adgo for his valuable scientific comments and guidance during the experimental stage of the research and for critically shaping the thesis. My special heart felt thanks also goes to my Co-Advisor, Dr. Tesfahun Kebede, for his close fatherly approach, guidance, coordination, valuable comments, suggestions and encouragement.

I gratefully acknowledge the teaching and research facilities afforded by the Department of Chemistry, Haramaya University, during the entire period of the sudy. I would also like to thank Dr. Endale Teju for his role as a postgraduate program coordinator and in making things smooth to make my stay in the department great.

The financial support from Research and Extension Office of Haramaya University **(***HURG/2015-03-02***)** is duely acknowledged.

Last but not least, I wish to thank my family and friends for their moral support, consistent encouragement and valuable advice.

TABLE OF CONTENTS

Continued

Continued

LIST OF TABLES

Tables **Pages**

LIST OF FIGURES

Figures **Pages**

LIST OF TABLES IN THE APPENDIX

Appendix Tables pages

LIST OF FIGURE IN THE APPENDIX

Appendix Figures Pages

Synthesis and Characterization of PANI/ZnO Based Electrochemical Sensor for the Detection of Some Toxic Heavy Metal Ions

ABSTRACT

A polyaniline/Zinc oxide (PANI/ZnO) nanocomposites based electrochemical sensor was Prepared by electropolymerization of ananiline monomer on a Zinc oxide film modified glassy carbon electrode (ZnO/GCE) at different film thickness to form PANI/ZnO/GCE. The electrochemical behaviour of the PANI film on bare and ZnO modified GCE was characterized by cyclic voltametry(CV) in monomer free 1.0 M HCl(aq) and EIS. CV of PANI on bare and ZnO modified glassy carbon electrode revealed two anodic and cathodic peaks. For comparison PANI and PANI/ZnO nanocomposites were also prepared chemically by *employing in-situ oxidation polymerization method and characterized by Uv−vis, FT-IR, HR-SEM and HR-TEM. Similarily, chemically produced nanomaterials characterized electrochemically showed two anodic and two cathodic peaks by CV in monomer free 1.0 M HCl(aq). The PANI/ZnO/GC electrode was employed as sensor for the detection of toxic heavy metal ions in water samples using* Ostroyoung *square wave anodic stripping voltammetry (OSW−ASV). The results indicated that the PANI-ZnO/GCE sensor was more sensitive (with a dynamic linear range of 5.0 to 25.0* ppb *and a detection limit (LOD) of* 2.8, 1.84, 0.21 and 0.84 ppb for *Cd(II), Pb(II), As(III) and Hg(II), respectively) than PANI/GCE and/or GCE. PANI-ZnO/GCE as sensor exhibited lower detection limits than the WHO permissible level of 5, 5, 10 and 5 μgL^{-1} for Cd(II), Pb(II), As(III) and Hg(II), respectively in water. All the detections were performed under optimized experimental conditions.*

Keywords: *Sensors, PANI/ZnO, Nanocomposite, Heavy metals, Toxicity, Cyclic Voltametry*

1. INTRODUCTION

Water pollution by toxic heavy metal ions (THMIs) is a global problem that needs attention owing to the persistence and toxicological effects to human health. Toxic heavy metal ions largely originate from anthropogenic activities such as mining, smelting of metal ores and from different kinds of waste products (March *et al.,* 2015). The HMIs such as Cadmium (Cd), lead (Pb), arsenic (As) and mercury (Hg) have been associated with health problems (cancers, skin lesion, cardiovascular diseases) and other diseases. Owing to the high toxicity of these metal ions in water, their provisional levels were set to be 10 μg/L (Cd), 0.5 μg/L (Pb), 10 μg/L (As) and 0.5 μg/L (Hg) (Kaur *et al.*, 2015). Since quality of our limited water resource is increasingly under threat by these metals, it is of paramount importance to monitor their level of concentration in water by using cost-effective, sensitive and selective techniques.

Various techniques have been developed for the detection of toxic and heavy metal ions. For example, traditional analytical/spectroscopic methods such as atomic absorption spectrometry, atomic emission Spectrometry (Durkalec *et al.,* 2015), inductively coupled plasma mass spectrometry [ICP – MS] (Bayon *et al.,* 2003) and atomic fluorescence spectrometry (AFS) (Sierra *et al*., 2013) or cold vapor atomic fluorescence spectrometry [CVAFS] (Zhang *et al.,* 2015) have been widely used for the detection of heavy metal ions. These techniques can simultaneously detect different ions with high sensitivity, selectivity and accuracy. However, it requires relatively expensive instrument and specialized personnel to carry out the operational procedures. Due to the capability of short analytical time, low power cost, high sensitivity and easy adaptability for in-situ measurement electrochemical detection methods have attracted great interest in the detection of HMIs (Wong *et al.,* 2007).

Mercury electrodes have been employed in the electrochemical detection of THMIs up to ppb levels. However, owing to the toxicity and tedious experimental precautions when working with mercury, its use has seriously declined and being discouraged. The toxicity of mercury electrodes has stimulated the quest for other materials or electrodes with low toxicity. Examples of such electrodes include gold electrode, boron doped electrode, silver electrode, glassy carbon electrode, carbon paste electrode, graphite electrode and bismuth film electrodes (Bia *et al.,* 2014).

In the area of electrochemistry, electrodes are usually modified with surface active layers such as conductive polymers, inorganic oxides or hybrid materials for various applications (Inzelt, 1994; Bard *et al.,* 2001). These modified electrodes can be prepared in several different ways, such as irreversible adsorption, covalent attachment of a monolayer, and coating the electrode with films of polymers (electrodepositing, spin coating, drop coating, spraying and electropolymerisation) on a substrate to produce an electrode suited to a particular function, whose properties are different from those of the unmodified substrate (Bard *et al.,* 2008).

One of the most interesting application areas of modified electrodes are in sensors. An electrochemical sensor is a small device that can be used for direct measurement of the analyte in the sample matrix. Ideally, such a device is capable of responding continuously and reversibly and does not perturb the sample (Bard *et al.,* 2001). The composition of chemically selective layer is of crucial importance for the construction and functioning of the sensor, as it also determines the effectiveness of the sensor. It further controls the selectivity, sensitivity, and lifetime and response time of the sensor (Diamond, 1998).

Conducting polymers such as polypyrrole, polythiophene, polyaniline and polynapthalene, have been used as electrode modifier for various applications. They have become interesting materials, because of their prospect applications in different types of electrochemical devices such as photovoltaic cells, batteries, sensors, super capacitors, electrochromic devices (Granstroem *et al.,* 1997) and smart devices (De Luca *et al.,* 2013). Common to all the conducting polymers, the conjugated π-electron system along the organic polymer chain is responsible for the conduction mechanism. Conducting polymers are capable of functioning as electron transfer mediators and redox changes are not localized at a specific center but are rather delocalized over a number of conducting polymer groups. Conducting polymer films can be formed on an electrode surface from solutions of monomer usually by electropolymerization. In addition to this polymer films can be formed on the electrode using methods that start with dissolved polymer include cast or dip coating, spin coating, electrodeposition, and covalent attachment via functional groups (Bard *et al.,* 2008).

Among conducting polymers, polyaniline has become the most attractive material because of the presence of the reactive –NH– groups in polymer chain (Stejskal *et al.,* 2010) and its broad

potential applications such as batteries (Gurunathan *et al.,* 2003), sensors (Deng *et al.*, 2003;Deshpande *et al.,* 2009), electronic devices (Jia *et al.*, 2002), super capacitors (Peng *et al* ., 2008), and corrosion protection in organic coatings (Olad *et al.,* 2011; Behzadnasab *et al.,* 2 011). Moreover, PANI possesses good electrical conductivity, high environmental stability, low cost (Zhang *et al*., 2007), light weight, flexibility, facile fabrication and possibility of both chemical and electrochemical syntheses (Patil *et al.,* 2006; Sharma *et al*., 2009). These unique properties make polyaniline more attractive by many research groups.

In recent years synthesis and characterization of nanostructured metal oxide/conducting polymer hybrid materials have been reported by many research groups because of their ability to detect organic and inorganic pollutants in the environment and their potential use as electrochemical sensors. Inorganic materials that can form composite with conducting polymers are metal oxides, clays, and zeolites which can be deposited on electrode surfaces. The interesting features of these films are they frequently show well-defined structures (e.g they have unique pore or interlayer sizes). These nanocomposites exhibit many new characters, such as electrical, optical, catalytic and mechanical (Sharma *et al*., 2009).

Zinc oxide (ZnO), one of the II-VI semiconductor materials, has attracted considerable interest because of its interesting properties such as wide band gap (approximately 3.37 eV), and long-term stability. ZnO has been applied in various applications, such as in light-emitting diode, gas and chemical sensors, solar cell, and biomolecular sensors. ZnO nanostructures have been frequently used for electrochemical sensor purpose since the large surface-to-volume ratio property leads to an improved signal-to-noise ratio, faster response times, enhanced electroa-nalytical performance, and increased sensitivity (Batista *et al*., 2005; Kang *et al*., 2005). In addition to this, ZnO nanostructures have unique biological advantages including non-toxicity, biosafety, bio-compatibility, and high electron communication features, which make them one of the most promising materials for electrochemical sensor or/and biosensor applications (Alimujiang *at el.,* 2010).

Zinc oxide nanoparticles have been prepared by using various techniques such as the aqueous hydrothermal growth, Sol–gel method, precipitation method,metal-organic chemical vapor deposition, electrochemical deposition methods and vapor–liquid-solid method. Among these

methods,the precipitation method is an easy and convenient method forthe preparation of ZnOnanoparticles (Lanje *et al*., 2013; Nehal *et al.,* 2015).

Some PANI–metal oxides nanocomposites were reported, for examples PANI/SnO_2 and PANI/TiO_2 (Xu *et al.,* 2005; Mo *et al.,* 2008; Shi *et al.,* 2009) to the best of our knowledge, only limited investigations are available in literature for the synthesis and characterization ZnO-PANI hybrid materials or PANI-ZnO at various film thickness to use as electrochemical sensor for the detection of toxic heavy metals (Cd, Pb, As and Hg) in water sample. The conducting polymer/ZnO on glassy carbon electrode can detect heavy metals from aqueous solution and greatly increasing the sensitivity of its determination and wide operative linear range of concentrations of toxic heavy metals.

Therefore, in this work, PANI films at different thickness were formed on bare and ZnO/GCE surface from solutions of anilinemonomer in acidic medium usually by electropolymerizationmethode. For PANI and PANI/ZnO nanocomposite were prepared chemically by employing in − situ oxidation polymerization method. The products were characterizedby Uv − vis, FT-IR, HR-SEM, HR-TEM, EDX analyizer, CV and EIS. The aim of the production of PANI-ZnO/GCEwasto apply as electrochemical sensor for the detection of toxic and heavy metalsions (Cd^{2+}, Pb^{2+}, As^{3+}, Hg^{2+}) in ground water samples.

OBJECTIVE OF THE STUDY

General Objective

To develop PANI/ZnO nanostructured electrochemical sensor for the detection of trace level of toxic heavy metals ions (Cd^{2+}, Pb^{2+}, As^{3+} and Hg^{2+}) in water sample collected from Midegha Woreda, Eastern Hararghe Zone, Oromia Regional State, Ethiopia.

Specific objectives

- To synthesize ZnO and PANI nanoparticles and PANI/ZnO nanocomposites by using *precipitation* and *in-situ oxidation polymerization method*, respectively;
- To synthesize PANI films electrochemically at various thickness on bare and ZnO nanoparticles modified GCE using potentiodynamic methods;
- To characterize structural and morphological properties of chemically as synthesized nanomaterials using Uv-vis, FT-IR, HR-SEM, HR-TEM and EDX analysis spectroscopic techniques;
- To investigate the electrochemical properties of the PANI/GCE and PANI-ZnO/GCE using CV and EIS;
- To optimize experimental condition (pH, deposition times and deposition potential) by using PANI-ZnO/GCE sensor for the detection of THM ions;
- To apply PANI-ZnO/GCE electrochemical sensor for the detection of THMI (Cd^{2+}, Pb^{2+}, As^{3+} and Hg^{2+}) in ground water sample employing OSW-ASV electrochemical techniques.

2. LITERATURE REVIEW

2.1. Toxic Heavy Metals

Heavy metals are defined as those elements with a specific density at least five times the specific gravity of water. Heavy metals include Cd, Cu, Pb, Zn, As, Ag, Cr, Fe, Pt and Hg group elements. Heavy metals are not biodegradable andtend to accumulate in living organisms, causing various diseases and disorders (Jang *et al*., 2008). Keep in mind that, among HMs, although some are necessary for life at low concentrations (Fe, Se, Co, Cu, Mn, Mo, Zn), unfortunately, many others are toxic even in low concentrations like (Hg, Pb, As, Cd). For sanitary reasons, it has become necessary to detect and quantify HMs in soil or in water. The most commonly found heavy metals in waste water include arsenic, cadmium, chromium, copper, lead, nickel, mercury and zinc, all of which cause risks for human health and the environment (Lambert *et al.*, 2000). And their toxicity is a problem of increasing significance for ecological, evolutionary, nutritional and environmental reasons. This toxicity is hazardous as they can accumulate in soil, and finally lead to water contamination (Moris *et al.*, 1995).

Therefore, the detection of toxic heavy metals cation in waste water has received many attentions in recent times. Because of their dangerous tendency to bio-accumulation, means an increase in the concentration of a chemical in a biological organism over time, compared to the chemical's concentration in the environment. Compounds accumulate in living things any time they are taken up and stored faster than they are broken down or excreted (Tsoumbaris *et al.*, 1994).

2.1.1. Arsenic and Its Toxicity

Arsenic is one of the most important heavy metals causing disquiet from both ecological and individual health standpoints (Hughes *et al.*, 1988). It has a semi – metallic property, is prominently toxic and carcinogenic, and is extensively available in the form of oxides or sulfides or as a salt of iron, sodium, calcium, copper, *etc.* (Singh *et al.*, 2007). Arsenic is the twentieth most abundant element on earth and its inorganic forms such as arsenite and arsenate compounds are lethal to the environment and living creatures. Humans may encounter arsenic by natural means, industrial source, or from unintended sources. Drinking water may get

contaminated by use of arsenical pesticides, natural mineral deposits or inappropriate disposal of arsenical chemicals. Deliberate consumption of arsenic in case of suicidal attempts or accidental consumption by children may also result in cases of acute poisoning (Saha *et al.*, 2006; Mazumder, 2008). Arsenic is a protoplastic poison since it affects primarily the sulphydryl group of cells causing malfunctioning of cell respiration, cell enzymes and mitosis (Gordon and Quastel, 1948).

Mechanism of Arsenic Toxicity

In arsenic biotransformation, harmful inorganic arsenic compounds get methylated by bacteria algae, fungi in humansto give monomethylarsonic acid (MMA) and dimethylarsinic acid (DMA). In this biotransformation process, these inorganic arsenic species (iAs) are converted enzymetically to methylated arsenicals which are the end metabolites and the biomarker of chronic arsenic exposure.

$$\text{iAs(V)} \rightarrow \text{iAs(III)} \rightarrow \text{MMA(V)} \rightarrow \text{MMA(III)} \rightarrow \text{DMA(V)}$$

Biomethylation is a detoxification process and end products are methylated inorganic arsenic such as MMA(V) and DMA(V), which are excreted through urine are bioindication of chronic arsenic exposure. However MMA(III) is not excreted and remains inside the cell as an intermediate product. Monomethylarsonic acid (MMA III), an intermediate product, is found to be highly toxic compared to other arsenicals, potentially accountable for arsenic-induced carcinogenesis (Singh *et al.*, 2007).

2.1.2. Cadmium and Its Toxicity

Cadmium is the seventh most heavy metal. It is a by-product of zinc production which humans or animals may get exposed to at work or in the environment. Once this metal gets absorbed by humans, it will accumulate inside the body throughout life. This metal was first used in World War I as a substitute for tin and in paint industries as a pigment. In today's scenario, it is also being used in rechargeable batteries, for special alloys production and also present in tobacco smoke. About three-fourths of cadmium is used in alkaline batteries as an electrode component, the remaining part is used in coatings, pigments and plantings and as a plastic stabilizer. Humans may get exposed to this metal primarily by inhalation and ingestion and

can suffer from acute and chronic intoxications. Cadmium distributed in the environment will remain in soils and sediments for several decades. Plants gradually take up these metals which get accumulated in them and concentrate along the food chain, reaching ultimately the human body. Cadmium is predominantly found in fruits and vegetables due to its high rate of soil-to plant transfer (Satarug *et al.*, 2011). Cadmium is a highly toxic nonessential heavy metal that is well recognized for its adverse influence on the enzymatic systems of cells, oxidative stress and for inducing nutritional deficiency in plants (Irfan *et al.*, 2013).

Mechanism of Cadmium Toxicity

The mechanism of cadmium toxicity is not understood clearly but its effects on cells are known (Patrick, 2003). Cadmium concentration increases 3,000 fold when it binds to cysteine rich protein such as metallothionein. In the liver, the cystein-metallothionein complex causes hepatotoxicity and then it circulates to the kidney and gets accumulated in the renal tissue causing nephrotoxicity. Cadmium has the capability to bind with cystein, glutamate, histidine and aspartate ligands and can lead to the deficiency of iron (Castagnetto *et al.*, 2002). Cadmium and zinc have the same oxidation states and hence cadmium can replace zinc present in metallothionein, thereby inhibiting it from acting as a free radical scavenger within the cell.

2.1.3. Lead and Its Toxicity

Lead is a highly toxic metal whose widespread use has caused extensive environmental contamination and health problems in many parts of the world. The various sources of lead such as (metal plating ,wastes from battery industries, Soil wastes, exhaust from automobiles, additives in gasoline and pigment, Factory chimneys, Smelting of ores, Fertilizers and pesticides) pollution in the environment (Sharma and Dubey, 2005). Hence human exposure of lead in the general population is either due to food or drinking water. Some is taken up by plants, fixation to soil and flow into water bodies, hence human exposure of lead in the general population is either due to food or drinking water (Goyer, 1997). Lead is an extremely toxic heavy metal that disturbs various plant physiological processes and unlike other metals, such as zinc, copper and manganese, it does not play any biological functions. A plant with high lead concentration fastens the production of reactive oxygen species (ROS), causing lipid

membrane damage that ultimately leads to damage of chlorophyll and photosynthetic processes and suppresses the overall growth of the plant (Najeeb *et al.*, 2014). Lead is capable of inhibiting the growth of tea plant by reducing biomass and debases the tea quality by changing the quality of its components (Yongsheng *et al.*, 2011). Even at low concentrations, lead treatment was found to cause huge instability in ion uptake by plants, which in turn leads to significant metabolic changes in photosynthetic capacity and ultimately in a strong inhibition of plant growth (Mustafa *et al.*, 2012).

Mechanisms of Lead Toxicity

Lead metal causes toxicity in living cells by following ionic mechanism and that of oxidative stress. The oxidative stress in living cells is caused by the imbalance between the production of free radicals and the generation of antioxidants to detoxify the reactive intermediates or to repair the resulting damage. Antioxidants, as *e.g.* glutathione, present in the cell protect it from free radicals such as H_2O_2. Under the influence of lead, however, the level of the ROS increases and the level of antioxidants decrease.

Another biomarker for oxidative stress is lipid peroxidation, since the free radical collects electron from lipid molecules present inside the cell membrane, which eventually causes lipid peroxidation (Flora *et al.*, 2012; Wadhwa *et al.*, 2012). At very high concentrations, ROS may cause structural damage to cells, proteins, nucleic acid, membranes and lipids, resulting in a stressed situation at cellular level (Mathew *et al.*, 2011). The ionic mechanism of lead toxicity occurs mainly due to the ability of lead metal ions to replace other bivalent cations like Ca^{2+}, Mg^{2+}, Fe^{2+} and monovalent cations like Na^{+}, which ultimately disturbs the biological metabolism of the cell. The ionic mechanism of lead toxicity causes significant changes in various biological processes such as cell adhesion, intra- and inter-cellular signaling, protein folding, maturation, apoptosis, ionic transportation, enzyme regulation, and release of neurotransmitters. Lead can substitute calcium even in picomolar concentration affecting protein kinase C, which regulates neural excitation and memory storage (Flora *et al.*, 2012).

2.1.4. Mercury and Its Toxicity

Mercury has no positive role in the human body, in fact a safe level of mercury exposure is very difficult to determine. It is a naturally occurring metal which is a shiny silver-white,

odorless liquid and becomes colorless and odorless gas when heated. Mercury is very toxic and exceedingly bioaccumulative. Major sources of mercury pollution include anthropogenic activities such as agriculture, municipal wastewater discharges, mining, incineration, and discharges of industrial wastewater (Chen *et al.*, 2012).

Mercury exists mainly in three forms: metallic elements, inorganic salts and organic compounds, each of which possesses different toxicity and bioavailability. These forms of mercury are present widely in water resources such as lakes, rivers and oceans where they are taken up by the microorganisms and get transformed into methyl mercury within the microorganism, eventually undergoing bio-magnifications causing significant disturbance to aquatic lives. Consumption of this contaminated aquatic animal is the major route of human exposure to methyl mercury (Trasande *et al.*, 2005).

Mercury is extensively used in thermometers, barometers, pyrometers, hydrometers, mercury arc lamps, fluorescent lamps and as a catalyst. It is also being used in pulp and paper industries, as a component of batteries and in dental preparations such as amalgams.

Mechanism of Mercury Toxicity

Mercury is well known as a hazardous metal and its toxicity is a common cause of acute heavy metal poisoning. Methylmercury is a neurotoxic compound which is responsible for microtubule destruction, mitochondrial damage, lipid peroxidation and accumulation of neurotoxic molecules such as serotonin, aspartate, and glutamate (Patrick, 2002).

Animals which are exposed to toxic mercury have shown adverse neurological and behavioral changes (Ashe *et al.*, 1953). The brain remains the target organ for mercury, yet it can impair any organ and lead to malfunctioning of nerves, kidneys and muscles. It can cause disruption to the membrane potential and interrupt with intracellular calcium homeostasis. Mercury binds to freely available thiols as the stability constants are high (Patrick, 2002).

Mercury vapors can cause bronchitis, asthma and temporary respiratory problems. Mercury plays a key role in damaging the tertiary and quaternary protein structure and alters the cellular function by attaching to the selenohydryl and sulfhydryl groups which undergo

reaction with methyl mercury and hamper the cellular structure. It also intervenes with the process of transcription and translation resulting in the disappearance of ribosomes and eradication of endoplasmic reticulum and the activity of natural killer cells. The cellular integrity is also affected causing free radical formation. The basis for heavy metal chelation is that even though the mercury sulfhydryl bond is stable and divided to surrounding sulfhydryl consisting ligands, it also contributes free sulfhydryl groups to promote metal mobility within the ligands (Bernhoft, 2011).

Table 1. Maximum permissible levels of toxic heavy metals in water

Toxic heavy metal in µg/L				Sources
Cd	Pb	As	Hg	
10	0.5	10	0.5	Kaur *et al.,* 2015
0.5	10	0.5	0.25	Ehi-Eromosele *et al.,* 2012
5	5	10	5	WHO, (2008)

2.2. Methods of Determination for Toxic Heavy Metals

Various analytical techniques have been developed for the detection of toxic and heavy metal ion in water, soil, plants. For example, traditional analytical methods such as [AAS, AES] (Durkalec *et al.,* 2015), [ICP – MS] (Montes – Bayon *et al.,* 2003) and atomic fluorescence spe ctrometry (AFS) (Sierra *et al.,* 2013) or [CVAFS] (Zhang *et al.,* 2015) have been widely used for the detection of heavy metal ions. These techniques can simultaneously detect different ions with high sensitivity, selectivity and accuracy. Another detection method is electrochemical detection methods have been used for the detection of toxic and heavy metal ion in a given sample with a short analytical time, low power cost, high sensitivity and easy adaptability for in-situ measurement (Wong *et al.,* 2007).

2.2.1. Spectroscopic and Chromatographic Methods

Several spectroscopic methods have been developed to monitor the levels of heavy metals in man, fossil fuels and environment. They include; flame atomic absorption spectrometry (FAAS), atomic emission spectroscopy (AES), graphite furnace atomic absorption spectrometry (GFAAS), inductively coupled plasma-atomic emission spectroscopy

(ICP/AES), inductively coupled plasma mass spectrometry (ICP/MS), x-ray fluorescence spectroscopy (XRFS), isotope dilution mass spectrometry (IDMS), electrothermal atomic absorption spectrometry (ETAAS) etc. Also other spectroscopic methods have been used for analysis of the quality composition of the alternative fuels such as biodiesel. These include Nuclear magnetic resonance spectroscopy (NMR), Near Infrared Spectroscopy (NIR), inductively coupled plasma optical emission spectrometry (ICP-OES) (Sierra *et al*., 2013).

THM have been determined by capillary gas chromatography using microwave induced plasma atomic emission spectrometer as the detector (Lobiniski and Adams, 1993). With the development of high performance liquid chromatography (HPLC) and other chromatographic techniques, a variety of separation modes have been employed to distinguish among deferent species, followed by calorimetric, spectroscopic, or electrochemical detection of the separated species (Le *et al.*, 1994; Hagege *et al.*, 1995).

2.2.2. Sensors

A sensor is a device, which is composed of an active sensing material with a signal transducer that detects and responds to some type of input from the physical environment. The role of these two important components in sensors is to transmit the signal without any amplification from a selective compound or from a change in a reaction (Bard *et al.*, 2008). These devices produce any one of the signals electrical, thermal or optical output signals which could be converted in to digital signals for further processing. One of the ways of classifying sensors is done based on these output signals. Among these, electrochemical sensors have more advantage over the others because; in these, the electrodes can sense the materials which are present within the host without doing any damage to the host system. On the other hand, sensors can be broadly classified in to two categories as chemical sensors and biosensors. Combination of these two different ways of classifications has given rise to a new type of sensors which are called electrochemicalbiosensors, wherethe electrochemicalmethods are applied for the construction and working of a biosensor (Balasubramanian *et al*., 2006)

2.2.2.1. Biosensors

Biosensors operate on the direct spatial coupling of an immobilized biologically active compound with a signal transducer and an electronic amplifier (Scheller *et al.*, 1992; Karube

et al., 2000). A biosensor can be defined as: *"a compact analytical device incorporating a biological or biologically derived sensing element either integrated within or intimately associated with a physicochemical transducer. The usual aim of a biosensor is to produce either discrete or continuous digital electronic signals that are proportional to a single analyte or a related group of analytes."* (Jin *et al.*, 2002; Keane *et al*., 2002).

Within these sensors, the active sensing material on the electrode should act as a catalyst and catalyze the reaction of the biochemical compounds to obtain the output signals (Vasantha *et al.*, 2006). The electrochemical methods are applied for the construction and working of a biosensor and/or electrochemical sensor (Wang, 2003 and Zhang, 2004). Biosensors are currently used to replace conventional analytical methods of sample analysis, which tend to be complicated, time consuming, expensive and not suitable for *in situ* monitoring (Kukla *et al*., 1999). Electrochemical biosensors are finding numerous applications in the field of clinical diagnosis, drug discovery, and detection of environmental pollutants, biotechnology, military and civil defense due to their smart size, quick and dependable response compared to the conventional systems and as well as electro active species generation (Lei *et al.*, 2007).

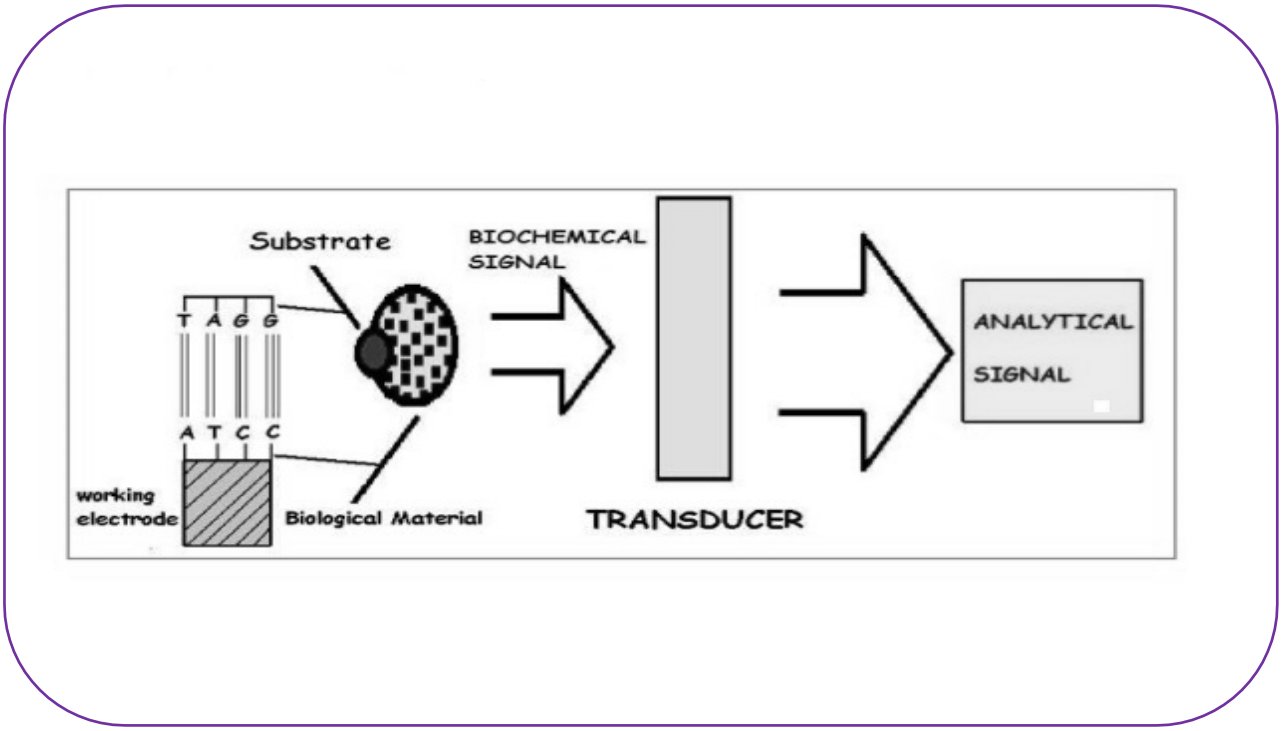

Figure 1. Schematic diagram showing the functioning of a biosensor device

2.2.2.2. Chemical sensors

A chemical sensor is different from a physical transducer in that it provides the user with information about the chemical nature of its environment. This sensor may consist of a physical transducer (e.g. a thermistor or piezo-electric crystal), or reference electrode (e.g. Ag/AgCl wire) at its core, and a chemically selective membrane, film or layer at the sensing tip. A chemical sensor is defined as: *"a device which furnishes the user with information about its environment; it consists of a physical transducer and a chemically selective layer"* (Diamond, 1998).

Chemical sensors have been widely used in such applications as critical care, safety, industrial hygiene, process controls, product quality controls, human comfort controls, emissions monitoring, automotive, clinical diagnostics, home safety alarms, and, more recently, homeland security. Chemical sensors can be classified into various groups according to their operating principle of the transducer. On the basis of the transducing element, they are categorized as electrochemical sensors, optical sensors, piezoelectric sensors and thermal sensors. Among all these chemical sensors, electrochemical sensors present an important subclass in which an electrode is used as a transducer (Yin *et al.*, 2009).

2.2.2.3. Electrochemical sensors

An electrochemical Sensor is a small device that can be used for direct measurement of the analyte in the sample matrix. Ideally, such a device is capable of responding continuously and reversibly and does not perturb the samples (Bard *et al.,* 2008). Electrochemical sensors as the subclass of chemical sensors in which an electrode is used as the transduction element, and are highly qualified for meeting the size, cost, and power requirements of on-site environmental monitoring (Taillefert *et al.*, 2000 and Wang, 2000). Such devices have found a vast range of important applications in the fields of clinical, industrial, environmental monitoring and agricultural analyses (Taillefert *et al.*, 2000).

2.3. Electrochemical Sensor and Their Working Principles

The working principle of electrochemical sensors is that an electro-active analyte is subjected to fixed or varying potential of some predefined patterns causes oxidation or reduction of analyte on the working electrode surface, which leads to the generation of an electrochemically measurable signal. This signal can be measured by the electrochemical detector. The working of electrochemical sensors is mainly based on the use of receptor element retained in direct contact with an electrochemically active transducer (electrode) to obtain an analytically useful signal by coupling chemical and electrochemical interactions (Aldridge,1950).

2.4. Types of Electrochemical Sensors

In recent times various types of electrochemicalsensors exist, depending on the method of operation and the field of application. On the basis of electrical signal which is recorded, electrochemical sensors can be divided into potentiometric sensors, amperometric sensors, and conductometric sensors which have a number of interesting applications in the areas of environmental, industrial, agricultural and clinical analyses (Janata, 2001).

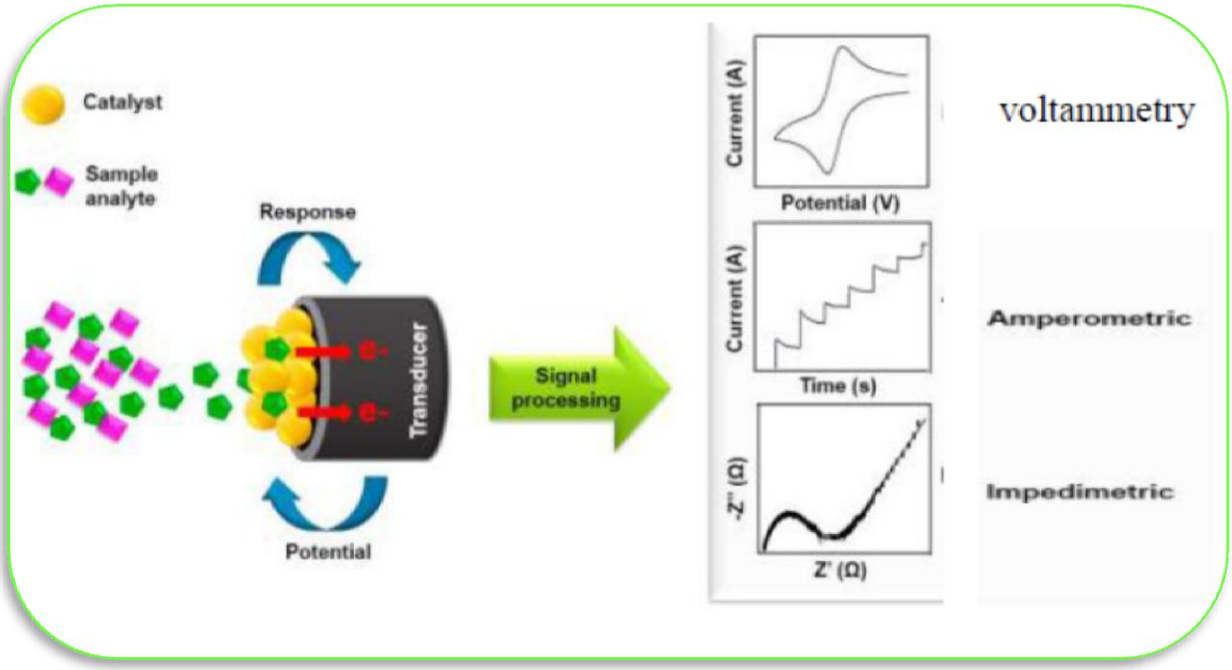

Figure 2. Schematic illustration of general principle of electrochemical sensing of HMs

2.4.1. Amperometric Sensors

The sensor responds to an analyte in a sample and interprets its concentration as an electrical signal via a chemical system connected to an electrochemical transducer. Amperometric sensors are based on heterogeneous electron transfer reactions that are both the oxidation and reduction of electro-active substances. If there is an increase in the overvoltage, i.e. the deviation from the redox potential, the rate of the heterogeneous charge transfer process is enhanced so as to cause the rate of the whole process to become controlled by mass transfer. If these conditions exist, the diffusion current, *Id*, is proportional to the concentration of the substance to be determined, *S0*, giving the following equation:

$$I_d = nAFD_0\frac{S_0}{\delta}$$

2.4.2. Potentiometric Sensors

In the functioning of Potentiometric sensor, a general operating condition of near-zero current flow is maintained and it measures the difference in potential between the working electrode and the reference electrode. The transducer may be an ion selective electrode (ISE), which is an electrochemical sensor, based on thin films or selective membranes as recognition materials. The output of a potentiometric sensor is a potential difference as a function of time. The simplest potentiometric technique is based on the concentration dependence of the potential, *E*, at reversible redox electrodes according to the Nernst equation:

$$E = E_0 + \frac{RT}{nF}\log_e(\frac{C_0}{C_R})$$

Where, E_0= standard redox potential T= absolute temperature n= N^{o} of exchanged electrons of the substance S a_s= activity of the substance S.

2.4.3. Conductometric Sensors

In the operation of conductometric sensors, sensing is based on measuring the time dependence of the change in conductivity as a result of the receptor recognition of its complimentary analyte. The measuring signal reflects the migration of all ions in the film (Hou, 2005). Conductometric methods of measurement make use of non-Faradaic currents. It operates on an alternating current of low amplitude and a frequency in the range of 1 kHz. The

measurement signal reflects the migration of all ions in the solution. This technique is therefore non-specific and may only be used for samples of identical conductivity. In conductometric membrane sensors the two electrodes are separated from the measuring solution by a gas-permeable membrane. The diffusion processes of the measured gases are the same as in gas sensitive ISEs (Scheller *et al.*, 1992).

2.5. Conducting Polymers (CP)

Conducting polymers such as polypyrrole, polythiophene, polyaniline and polynapthalene, has been used as electrode modifier for various applications. Conducting polymers (CPs) contain π-electron which is a backbone responsible for their unusual electronic properties such as electrical conductivity, low energy optical transitions, low ionization potential and high electron affinity. The extended π-conjugated systems of the CPs have single and double bonds alternating along the polymer chain (Gerard *et al.*, 2002). Conducting polymers are capable of functioning as electron transfer mediators and redox changes are not localized at a specific centre but are rather delocalized over a number of conducting polymer groups.

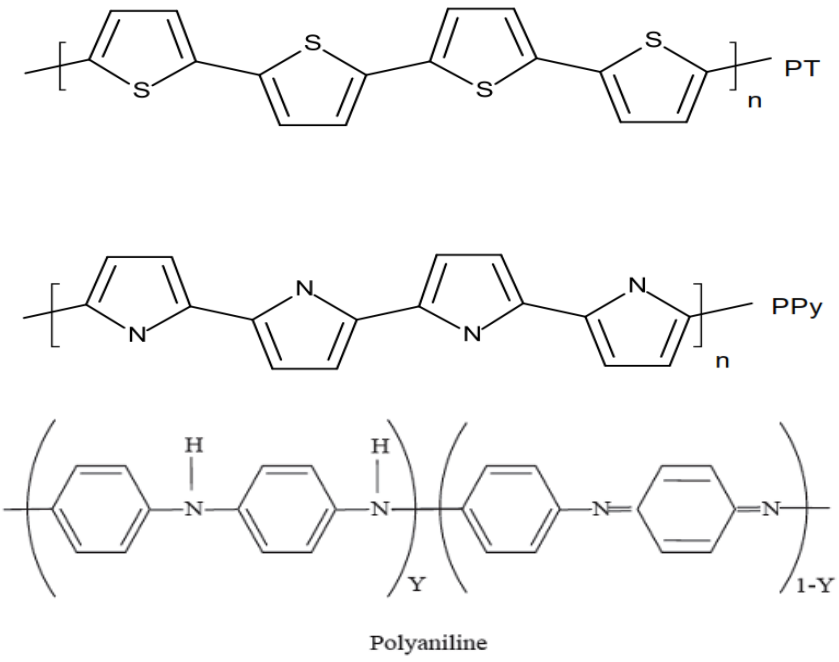

Figure 3. Some common conductive polymers

CPs show almost no conductivity in the neutral (uncharged) state but become electrically conductive upon partial oxidation or reduction, a process commonly referred to as ‘doping’. A

new class of polymers known as intrinsically conducting polymers or electro active conjugated polymers has recently emerged. They have become interesting materials, because of their prospect applications in different types of electrochemical devices such as photovoltaic cells, batteries, sensors, super capacitors, electrochromic devices (Granstroem *et al.,* 1997) and smart devices (De Luca *et al.,* 2013).

Conducting polymers can be synthesized either chemically or electrochemically. The most widely used technique is the oxidative coupling involving the oxidation of monomers to form a cation radical followed by coupling to form dications and the repetition leads to the polymer formation. Chemical synthesis is known to permit the scale−up of the polymers, which is currently not possible with electrochemical synthesis. However, electrochemical polymerization is the most preferred general method for preparing CPs because of its relatively straight forward synthetic procedure, simplicity and reproducibility. Generally, electrochemical polymerization can be carried out galvanostatically (constant current), potentiostatically (constant potential) or by potentiodynamically (potential scanning/cycling or sweeping) methods.

Conducting polymer films can be formed on an electrode surface from solutions of monomer usually by electropolymerization. In addition to this polymer films can be formed on the electrode using methods that start with dissolved polymer include cast or dip coating, spin coating, electro deposition, and covalent attachment via functional groups. By varying either the potential or current with time, the thickness of the film can be controlled. In this procedure, the monomers at the working electrode surface undergo oxidation to form radical cations that react with other monomers or radical cations, forming insoluble polymer chains on the electrode surface.

2.5.1. Conducting Polymers as Electrochemical Sensors for THMI

By polymerization of monomers and post-modification of polymerized products on electrodes, a large number of organic polymers, particularly conducting and chelating polymers, have been used to construction sensors. The most commonly used conducting polymer includes polyacetylene (PAc), polyaniline (PANI), polypyrrole(PPy), poly(p-phenylene)(PPP), polythiophene (PTh), and poly (3,4-ethylenedioxythiophene) (PEDOT) (Kumar *et al.*,2012; Manisankar *et al.,* 2008; Yasri *et al.,* 2011). Commonly they are combined with inorganic

nanomaterials to fabricate sensitive sensors for heavy metals. For example, with thiol groups of poly (2,5-dimercapto-1,3,4-thiadiazole) (PDMcT) to bind Cd^{2+} and Pb^{2+} (He *et al.*, 2011) combined PDMcT with MWCNTs to modify GCE for analysis of Cd^{2+} and Pb^{2+} binding ability of PDMcT and the function of MWCNTs, the limits of detection (S/N=3) for Cd^{2+} and Pb^{2+} were 0.03 and 0.05 μgL^{-1}, respectively.

2.5.2. Polyaniline as Electrochemical Sensor

Polyaniline (PANI) represents one of the most widely used conducting polymers. The general structure of PANI is shown in Figure 4, where (1-y) is the average oxidation state.

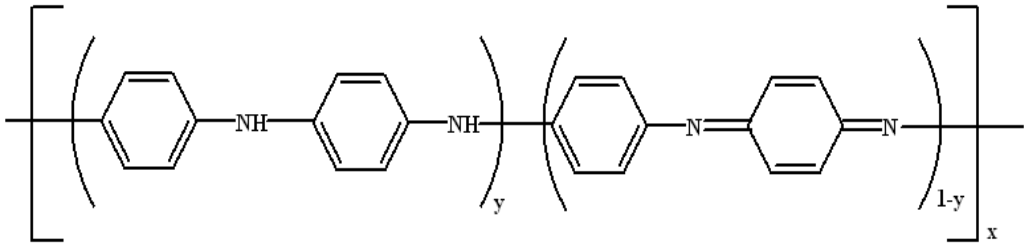

Figure 4. Structure of Polyaniline

Polyaniline (PANI) has been the most promising representative and several reasons account for that. Aniline as monomer is relatively inexpensive, the polymerization reaction proceeds with high yield and the polymerization of the monomer to polyaniline is straightforward. Formation of the radical cation of aniline by oxidation on the electrode surface (step 1) is considered to be the rate determining step. This is followed by coupling of radicals, mainly *N*- and *para*-forms, and elimination of two protons. The oligomer formed then undergoes oxidation on the electrode surface along with aniline. The radical cation of the oligomers couples with an aniline radical cation, resulting in propagation of the chain. The formed polymer is doped by the acid (HA) present in solution (step 4) (Wallace *et al*., 2003).

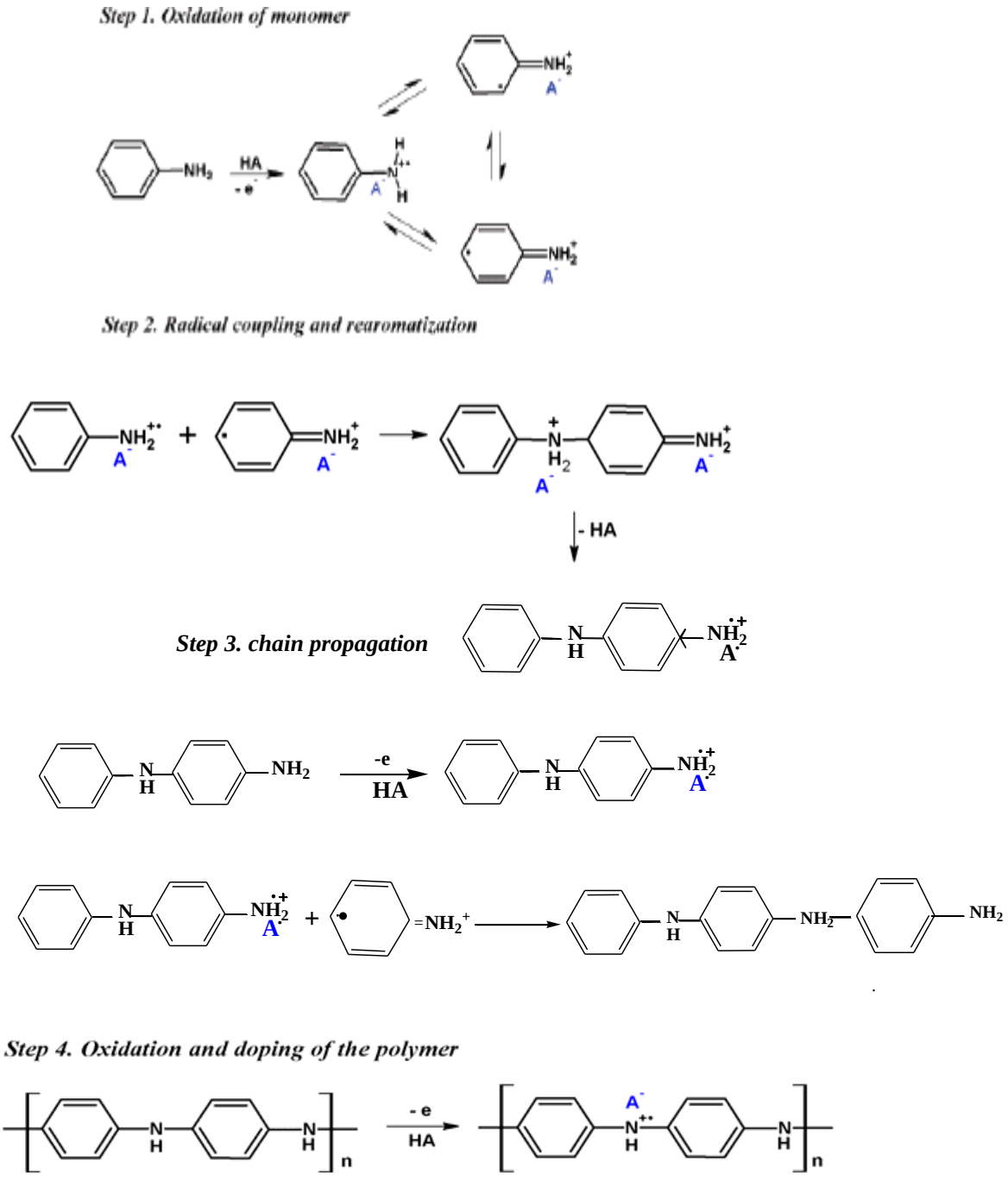

Figure 5. Electrochemical polymerization of aniline in presence of a dopant anion A^-

Recently assembly of organic layers onto surfaces has been widely used in constructing the electrochemical sensors due to their unique characteristics such as high surface area and strong adsorption ability. Some of the advantages of utilizing PANI-coated electrodes in sensors include impressive signal amplification and the elimination of electrode fouling (Sakthivel *et al.*, 1997).

2.6. Metal oxides as Electrochemical Sensors

Due to their interesting nanomorphological, functional bio-compatible, non toxic and catalytic properties nanostructured metal oxides such as TiO_2, SnO_2, ZnO, Fe_3O_4, NiO, ZrO_2, MgO and MnO_2 have been widely used in the detection of toxic and heavy metal ions. These materials exhibit enhanced electron transfer kinetics and strong adsorption capability. For example, porous MgO nano flowers have been synthesized to fabricate heavy metal sensitive electrode (Wei *et al.,* 2012). By combining with square wave anodic stripping voltammetry (SWASV), the modified electrode exhibits excellent sensing performance for Pb^{2+} and Cd^{2+} with detection limits of 2.1 pM and 81 pM, respectively.

2.7. Polyaniline/Metal Oxide Nanocomposite as Electrochemical Sensor

Due to their superior electrical conductivities, good adhesion properties and suitable structural characteristics conductive polymers (PANI) have received considerable attention for the detection of trace heavy metals ions (Zhu *et al.,* 2006). Due to its facile preparation, high conductivity and good environmental stability, the presence of the reactive –NH– groups in polymer chain, conductive polyaniline (PANI) can be electrochemically coated on the surfaces of glassy carbon electrode (GCE) and forms a porous coating. PANI deposited on electrode surfaces could enhance the stripping responses in the detection of metal ions in a given samples. PANI modified electrode exhibits excellent sensing performance for Cd^{2+} with R = 0.974 and DL = 0.13 μM and for Pb^{2+} with with R = 0.989 and DL = 0.1 μM by employed with square wave anodic stripping voltammetry (SWASV) (Wang *et al.*, 2011).

2.8. Synthesis Methods of Nanomaterials

2.8.1. Sol-Gel Method

(Bagotsky, 2006) Sol-gel technology is a well established colloidal chemistry technology, which offers possibility to produce various materials with novel, predefined properties in a simple process and at relatively low cost process. The gel can be considered as a solid macromolecule immersed in a solvent. Sol-gel process consists in the chemical transformation of a liquid (the sol) into a gel state and with subsequent post-treatment and transition into solid oxide material.

2.8.2. Hydrothermal Growth Method

In the solvothermal processes, the chemical reaction takes place in a sealed vessel such as bomb or autoclave, where solvents are brought to temperatures well above their boiling points. When water is used as solvent, it is called a hydrothermal process. It can create nanoparticles with high crystallin comparison between Sol-Gel Method and Hydrothermal growth ity and narrow size distribution high T and long reaction times (Zou *et al*., 2011).

Table 2. Comparison between Sol-Gel Method and Hydrothermal growth

Methods	Advantage	Disadvantage	References
Sol-Gel Method	➢ It can create NPs with powder ➢ Better homogeneity and phase purity	➢ Raw materials for this process is expensive	Bagotsky, 2000
Hydrothermal growth method	➢ It can create NPs with high crystalline ➢ It does not require Sop histicated equipment; ➢ It is low cost, environm ent friendly, and thus suitable for scale-up.	➢ Complex process control, reliability problems, Expensive and autoclaves	Zou *et al*., 2011 Chen *et al*., 2010. Byrap *et al*., 2005

2.8.3. Precipitation Method

Precipitationis a solid created from a solution. When the reaction occurs in a liquid solution, the solid formed is called the 'precipitate'. The chemical that causes the solid to form is called the 'precipitant'. Without sufficient force of gravity (settling) to bring the solid particles together, the precipitate remains in suspension.Precipitation can be used as a medium. The precipitate-free liquid remaining above the solid is called the 'supernate' or 'supernatant'. The formation of a precipitate indicates the occurrence of a chemical reaction. Precipitation mayoccur rapidly from a super-saturated solution. In solids, precipitation occurs if the concentration of one solid is above the solubility limit in the host solid, due to e.g. rapid

quenching or ion implantation, and the temperature is high enough that diffusion can lead to segregation into precipitates. Precipitation in solids is routinely used to synthesize nanoclusters (Dhara 2007). An important stage of the precipitation process is the onset of nucleation.

2.8.4. In-Situ Oxidation Polymerization Method

In a vast majority of cases, PANI is synthesized by *in situ oxidative polymerization* of aniline. *In situ* oxidative polymerization is used for the synthesis of polymeric (oligomeric) products from various classes of monomers (aromatic amines, phenols, thiophenols, aromatic hydrocarbons and heterocycles (Higashimura and Kobayashi, 2004). The monomers used in oxidative polymerization are characterized by pronounced electron donor properties and high oxidation tendency. These properties, in particular, are inherent to aromatic amines, phenols and thiophenols or sulphur- andnitrogen-containing heterocycles due to the presence of electron donor substituent in benzene or heterocyclic ring. Oxidation of monomer takes place under the action of inorganic (or organic) oxidizing agent or the applied potential. During this process, cation or cation radical sites are generated in monomer (polymer) molecule, thus initiating polymer growth.

2.8.5. Electrochemical PolymerizationMethod

Electrochemical polymerization - a solution of monomer is oxidized or reduced to an activated form that polymerizes to form a polymer film directly on the electrode surface. This procedure results in few pinholes since polymerization would be accentuated at exposed (pinhole) sites at the electrode surface. Unless the polymer film itself is redox active, electrode passivation occurs and further film growth is prevented (Tovidea, 2014).

2.9. Modification of Electrode Surface with Different Nanomaterials

2.9.1. Preparation of ZnO Thin Film-Coated Glassy Carbon Electrode

Electrodes (GCE) modified with surface active layers such as, inorganic oxides (ZnO nanoparticles) for various applications. These modified electrodes can be prepared by dropcoating the electrode with thin films of ZnO nanoparticles on a substrate to produce an electrode suited to a particular function, whose properties are different from those of the

unmodified substrate (Bard *et al.,* 2008).The electrochemical behaviour of ZnO modified GCE was examined by cyclic voltammetry(Babu and Narayanan, 2013; Bashami *et al*., 2015).

2.9.2. Electrodeposition of PANI Thin Film-Coated on GCE

Electrochemical polymerization is favorable, since in the most cases the polymer is directly deposited on the electrode to facilitating analysis. On the other hand, electrochemical polymerization is especially useful if polymer film electrode is needed (Wang *et al*., 2015).

2.10. Electrochemical Characterization Techniques

It is assumed for all the techniques discussed in this section that the analyte solution is quiet (i.e. stirred or unstirred) during the experimental performance, in order to ensure that mass transport by convection is absent. It is also assumed that an excess of ionic electrolyte has been added to the solution in order to ensure that mass transport by migration is also absent. The only form of mass transport remaining that will be considered is diffusion (Monk, 2001).

2.10.1. Cyclic Voltammetry (CV)

In voltammetry the root word “voltam-” refers to both potential (“volt-”) and current (“am-”). During any voltammetry experiment the potential of an electrode is varied while we simultaneously monitor the induced current. When cyclic voltammetry is performed, a solid electrode called the working electrode (WE) is employed. During an experiment the potential of the WE is ramped at a scan rate (v), and the resultant trace of current against potential is plotted in what is called a voltammogram (Monk, 2001).

Cyclic voltammetry is one of the most widely used electrochemical techniques for acquiring qualitative information about electrochemical reactions. The power of cyclic voltammetry results from its ability to rapidly provide considerable information on the thermodynamics of redox processes and the kinetics of heterogeneous electron transfer reactions and on coupled chemical reactions or adsorption processes (Mathebe, 2004).In cyclic voltammetry the potential is ramped from an initial potential (E_i) and at the end of its linear sweep, the direction of the potential scan is reversed, usually stopping at the initial potential. The potential may commence with further additional cycles. The potential at which the change in

direction occurs is also known as the switch potential (E_λ). The scan rate between E_i and $E_\lambda$is the same as that between E_λ and E_i and the values of the scan rate forward and reverse are always written with positive numbers. In Figure 6 a voltammograms for a simple solution-phase couple is shown and it is also known as a cyclic Voltammograms (Monk, 2001).

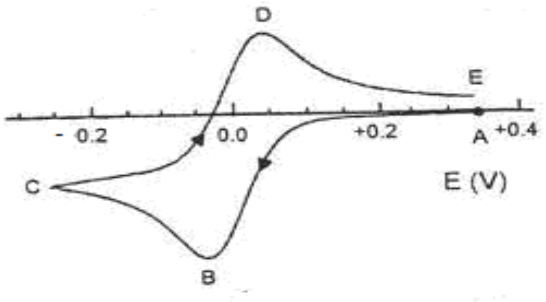

Figure 6. A typical cyclic voltammogram

In cyclic voltammetry, the position of both the cathodic and anodic peaks gives us thermodynamic information of the redox couple used. The anodic and cathodic peak potentials also enable you to calculate the formal electrode potential,$E^{o\prime}$, as follows

$$E^{o\prime} = \frac{E_{p,a} + E_{p,c}}{2}$$

The $E^{o\prime}$ (normally called the formal potential or the formal redox potential) is in concept similar to the standard electrode potential, E^{θ} (Monk, 2001; Zanello, 2003).

2.10.2. Square Wave-Anodic Stripping Voltammetry (OSW-ASV)

This technique involves the application of square wave modulation to a constant or nearly constant dc potential, and the current generated is sampled at the end of successive half cycles of the square wave. Three currents are generated i.e. forward current from the forward pulse (I_f), the reverse current from the reverse pulse (I_r) and that for the net current (I_d) which are then plotted against the potential on the corresponding staircase tread (Bard *et al.,* 2008).

The peak height is directly proportional to the concentration of the electroactive species and detection limit as low as 10^{-8} is possible. OSW-ASV has excellent sensitivity, the rejection of background current, high signal to noise ratio and applicability to a wider range of electrode

materials and systems (Kounaves, 2007 and Akinyenye, 2008). Square wave anodic stripping voltammetry can play very important role in the characterization of electroactive species with poor, overlapping or ill-formed redox signals in cyclic voltammetry by producing individual sharp peaks (Williams-Dottin, 2001). It can also be applied in study of the electrode kinetics and determination of some species at trace levels..

2.10.3. Electrochemical Impedance Spectroscopy (EIS).

Electrochemical Impedance Spectroscopy (EIS) is used to investigate the performance of the modified electrodes being an effective method of probing the features of a surface modified electrode. The charge transfer resistance of the CP coating increases with the increase of cycles. In the electrochemical impedance spectroscopy (EIS) there are two axes: the y-axis represents the negative number of the imaginary part of the measured impedance while the x-axis represents the real part of the measured impedance. For a reaction that is reversible, the Nyquist plot usually exhibits two regions: (i) a semicircle at a high frequency region which corresponds to electron charge transfer process from which the electron-transfer resistance value can be measured directly, and (ii) a straight line section at low frequency region of the plot, which represents the diffusion-limited transport of the redox species from the electrolyte to the electrode interface (Wang *et al.,* 2011).Regions of mass-transfer and kinetic control are found at low and high frequencies, respectively (Bard, 2008)

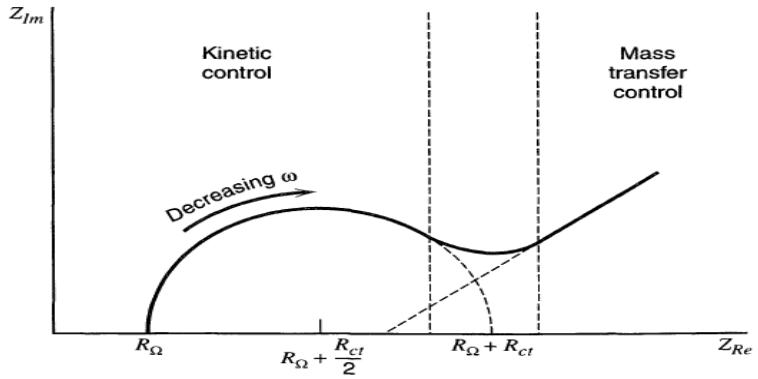

Figure 6.Impededednce plot for an electrochemical system.

3. MATERIALS AND METHODS

In this chapter sampling site and sampling techniques, experimental site, instrumentation, chemicals and reagents used are described. The synthesis of PANI, ZnO and PANI/ZnO nanocomposite electrochemical sensor on glassy carbon electrode and characterization outlined. This followed by preparation of standard solution and determination of Cd^{2+}, Pb^{2+}, As^{3+} and Hg^{2+} metal ions in water samples collected from Mideghe Woreda, Eastern Hararghe Zone, Ethiopia by using PANI-ZnO/GCE electrochemical sensor.

3.1. Sampling Site and Sampling Techniques

Ground-water Samples were collected form Mideghe Woreda, Eastern Hararghe Zone, Oromia Regional State, Ethiopia. It was noted that the water is usually used for drinking both for humans and animals and for irrigation by local communities. The water was collected from four sampling area in the district on the same day in 1000 mL volume plastic bottles previously cleaned by washing and rinsed with tap water and later soaked in 10% HNO_3 for 24 h and finally rinsed with de-ionized water prior to usage. During sampling, sample bottles were rinsed with sampled water three times and then filled with water sample at a depth of one meter below by submerging the plastic containers into the water. The water sample was stored in the refrigerator below 4^oC.

3.2. Experimental Site

Synthesis of the ZnO, PANI and PANI/ZnO nanocomposites, PANI and PANI/ZnO modified GCE, UV-vis characterization for as synthesized composites and CV, EIS and OSW-ASV electrochemical characterization of modified electrodes, buffers and standard solution preparation were conducted at Haramaya University, Department of Chemistry Research Laboratory. FT-IR characterization was done in Addis Ababa Science and Technology University department of chemistry laboratory. HR-TEM HR-SEM and EDX analysis were conducted at University of the Wester Cape, Department of Chemistry, Cape-Town, South Africa.

3.3. Apparatus and Instruments

Cyclic voltammetric (CV), Oyster Square Wave Anodic StrippingVoltammetry (OSW-ASV) and Electrochemical Impedance Spectroscopy (EIS) measurements were performed using BAS100B Electrochemical Bio-analyzer in three electrode cell arrangement using Windows™ software together with electrochemical workstation from Bio-Analytical Systems (BAS), Model BAS 100B product of USA. The reference electrode was calibrated with respect to the potassium hexacyanoferate in potassium chloride (2 mM $K_3Fe(CN)_6$. The three-electrode cell system was used. Glassy carbon electrode (3 mm diameter) was employed as a working electrode; a platinum wire and Ag/AgCl (saturated 3 M KCl) were used as counter and as reference electrode, respectively.

Infrared, Spectrum65 FTIR (PerkinElmer), UV-vis spectra (SANYO, SP65) measurements were recorded using (3 cm by 3 cm) quartz cuvettes with Nicolette Evolution 100 Spectrometer (Thermo Electron Corporation, UK). Other all materials and apparatus such as polishing pads obtained from Buehler, IL, USA, micropipettes, magnetic stirrers, sonicator, analytical balance (digital), sample holders, de-ionizer, 0.2 μm membrane (Whatman) filter paper, pH-meter, conical flasks, round bottom flasks, and beakers of various size and evaporating plate for heating were used.

3.4. Chemicals and Reagents

Aniline (99.8%, analytical grade) was obtained from Aldrich distilled before use , CH_3COOH (99.8%), HNO_3 (85%), Chloroform (99.8%), DMF (99.89%), ethanol (99.7%), CH_3COONa, KCl (99.99%), Na_2CO_3 (99%), $Zn(NO_3)_2.6H_2O$(99%), $Cd(NO_3)_2.4H_2O$ (99%), Pb(NO3), $Hg(NO_3)_2.H_2O$, As-Metal and $K_3Fe(CN)_6$ (95%), purchased from Merch were used as received. Hydrochloric acid (36.5%), APS (98%), methanol (99.8%) from Indian used without purification. Alumina micro powders (1.0, 0.3 and 0.05 μm) purchased from Böchler was used for polishing the GCE. All experimental solutions were purged with high purity of Argon (99.999%) obtained from (Merch, Germany) gas for about 5 minutes before running experiment and overflow the gas was maintained during the experiment to remove the dissolved oxygen.

3.5. Experimental Procedures

3.5.1. Chemical Synthesis Methods

3.5.1.1. Zinc Oxide nanoparticles

ZnO nanoparticles were prepared by *a precipitation method* (Lanje *et al*., 2013; Nehal *et al.,* 2 015). Two solutions were prepared: Solution A (0.1 mol of [$Zn(NO_3)_2.6H_2O$]) was prepared by dissolving 29.747 g of Zinc nitrate hexahydrate [$Zn(NO_3)_2.6H_2O$] in 200 ml distilled and deionized water; and solution B (0.12 mol Na_2CO_3) was prepared by dissolving 12.7188 g of sodium carbonate in 240 ml distilled water. After that, the precursor was prepared by adding solution A to solution B drop wise under vigorous stirring for 2 h. The precipitate resulting from the reaction between the two solutions was allowed to settle down for 24 h, filtered with 0.2 µm membrane filter (Whatman) and washed three times each with DI water and ethanol. The precipitate was dried at 100 ^oC for 6 h to form the precursor for ZnO. The precursor obtained, after drying, was calcined in air at 300 ^oC for 24 h in programmable furnace to get the nano-ZnO particles.

3.5.1.2. Synthesis of PANI nanoparticles

Synthesis of PANi by *in-situ oxidation polymerization method* (Alam *et al*., 2013).20 mL double distilled aniline with 1.0 M HCl in 250 mL round bottom flask at 27 ^0C was stirred for 30 minutes and subsequently 125 mL of 1.0 M APS (ammoniumpersuphate) solution was added drop wise. After the addition of APS, stirring of the reaction mixture was continuously carried out up to 4 h, resulting in thick green solution kept for 24 h. The precipitate was washed with 1 M HCl and ethanol to remove oligomers; the solution turned colourless and it was then dried in vacuum oven at 60 ^oC for 24 h to obtain green colored PANI (emeraldine). The product was labeled as nano-PANI particle.

3.5.1.3. Preparation of PANI–ZnOnanocomposites

Polyaniline–ZnO nanocomposites were prepared by *in-situ oxidation polymerization method* (Yerawa *et al*., 2012). Initially known wt. of ZnO (10%) was added to aniline prepared in aqueous hydrochloric acid (1.0 M) and stirred for half an hour, then allow settling down for another half an hour. To this solution, ammonium persulphate as an oxidant prepared in

aqueous hydrochloric acid (1.0 M) was added drop-wise for half an hour under constant stirring at 0–4 ^{o}C in presence of argon atmosphere. The monomer to oxidizing agent ratio was kept at 1:1.25. Stirring was continuing for 8 h, the resulting dark green mixture was kept over-night and then filtered. The precipitated polymer was washed with distilled water until the filtrate was colorless, then with ethanol and methanol to remove excess initiator, monomer and oligomers. Finally, the polymer was dried in air for about a day and then in an oven at 80 ^{o}C for 15 h. The product was labeled as PANI–ZnO nanocomposite.

3.5.2. Electrochemical Synthesis Method and Its Characterization

3.5.2.1. Electropolymerization and characterization of PANI/GCE

Electrochemical polymerization of polyaniline was carried out in a three-electrode cell in one compartment cell with glassy carbon (GC) as working electrode, Pt wire counter electrode and Ag/AgCl (saturated 3 M KCl) reference electrode. Before electropolymerization, solution were purged with argon and overflow of argon gas was maintained during electropolymerization. Prior to all the polymerizations the GC working electrodes was polished with 1, 0.3 and 0.05 μm alumina powder successively to get shiny surface and rinsed with distilled water followed by ultrasonication for 5 min with de-ionised water and ethanol and dried at room temperature. Electropolymerization was performed in a solution of 0.1 M aniline/1.0 M HCl aqueous solution at scan rate of 50 mVs^{-1} and 5, 10 and 15 cycles were taken for the characterization of the PANI film by cyclic voltammetry (CV) in monomer free aqueous solution of 1 M HCl electrolyte (Tovidea*, et al.*, 2014). The PANI as formed thin film on GC electrode was washed with deionised water before characterization by CV. The potential range was from -0.6 to + 1.10 V at scan rate of 5, 10, 25, 50, 75 and 100 mVs^{-1}. All experiments were performed at room temperature (20 ±2 ^{o}C).

3.5.2.2. GCE modified with ZnO and its characterization

Prior to film casting, the GCE was polished with alumina slurry. The polished electrode was sequentially sonicated in 10% HNO_3, then in ethanol:water (1:1) mixture; and finally, it was dried in air. The homogenous ZnO suspension was prepared by dispersing 1.0 mg ZnO powder in 1.0 mL of chloroform and sonicating for 15 min. The ZnO thin film was casted on the GCE surface, for preparation of ZnO/GCE, by spreading 5.0 μL of the ZnO suspension on

the flat surface of the electrode and drying at room temperature. The electrochemical behaviour of ZnO/GCE was examined by cyclic voltammetry. Thus ZnO/GCE shifted on to 0.1 M NaOH as a supporting electrolyte. The potential range was from -0.24 V to +1.245 V at scan rate of 50 mVs^{-1}. It can be seen that the ZnO is non electreactive in the selected potential region. However, itshows enhanced peak current than the bare GCE which indicated that the modified electrodecan be further used (Babu and Narayanan, 2013 and Bashami *et al*., 2015).

3.5.2.3. Electropolymerization and characterization of PANI-ZnO/GCE

Before electropolymerisation of PANI on ZnO/GCE, chemically produced ZnO was drop coated on GCE. After drying ZnO/GCE, PANI was elctropymerized first 5 potential cycles, second 10 and third 15 cycles in the solution of 0.1 M aniline/1.0 M HCl (aq) at scan rate of 50 mVs^{-1}. The PANI as formed thin film on ZnO/GCE electrode was washed with deionised water before characterization by cyclic voltammetry in monomer free aqueous solution of 1.0 M HCl electrolyte in the potential range −0.6 to +1.1 V and scan rate of (5, 10, 25, 50, 75 and 100) mVs^{-1}.

3.5.3. Cyclic Voltammetry of Chemical as Synthezed Nanomaterials

2 mg of PANI dissolved in 2 ml of DMF and ultrasoncated for 2 h. Then approximately 10 μL of the above suspension was then drop-coated onto the surface of a bare glassy carbon electrode and dried at room temperature. Similarly, 2 mg of PANI/ZnO was dissolved in 2 ml of DMF after sonication it was drop-coated on the bare electrode to obtain PANI/ZnO/GCE (Jain *et al.,* 2014). The PANI and PANI/ZnO thin film on GC electrode was washed with deionised water before characterization by CV. The potential range was from -0.6 V to +1.1 V at scan rate of (5, 10, 25, 50 and 75) mVs^{-1}.

3.6. Structural and Morphological Properties of Nanomaterials

ZnO, PANI and PANI/ZnO nanocomposite chemically synthesized samples were characterized using UV-visible; using SANYO, SP65 spectrophotometer, by scanning over 200-800 nm wavelength. The as synthesized samples were also characterized by FT-IR spectroscopy measured using Spectrum65 FT-IR (PerkinElmer) in the range 4000-400 cm^{-1}

and KBr pellets to assign functional groups of ZnO, PANI and PANI/ZnO. Morphological characterization was made employing by HR-SEM, EDX and HR-TEM.

3.7. Preparation of Acetate Buffer Solution

Acetate buffer was used as supporting electrolyte and made by mixing 79 mL of 0.1 M sodium acetate solution and 21 mL of 0.1 M CH_3COOH added slowly in 1000 mL volumetric flask. After the addition, the solution was diluted to 500 mL with de-ionized water and the pH was adjusted by adding 0.1 M HCl and 0.1 M NaOH to the pH of 5.2 using pH-meter.

3.8. Standard Solution Preparation

In the process of preparing and determining standard solutions and samples, deionized water was used throughout the experiments. All the glassware, beakers, flasks and measuring cylinders were first kept for 2 days in 6 M HNO_3, after which they were cleaned with distilled water. 1 g/L or 1000ppm of standard metal solutions of Pb(II), Cd(II), Zn(II) and Hg(II) were prepared as stock solution from the nitrates of the corresponding metals $Pb(NO_3)_2$, $Cd(NO_3).4H_2O$, $Zn(NO_3).6H_2O$ and $Hg(NO_3)_2$, respectively, whereas As(III) standard solution was prepared from As-metal. Five1000 mL volumetric flasks cleaned, labeled and half filled with deionized distilled water; 4.6 g $Zn(NO_3)_2.6H_2O$, 1.6 g $Pb(NO_3)_2$,1.7 g $Hg(NO_3)_2.H_2O$, 2.74 g $Cd(NO_3)_2.4H_2O$ and 1.0 g As-metal were accurately measured using analytical balance and added to prepare 1000mg/L of standard stock solution. 1 mL concentrated HNO_3 was added to each of the four volumetric flasks for dissolving the metals sample (acidification of the sample was required since higher acidity increases the ability of the metal ions to be dissolved in the water). After the salts are dissolved, the volumetric flasks were filled up to the mark with deionized distilled water. The calibration graph was drawn using standard solutions of concentrations of (0, 0.1, 0.5, 1, 2, 3, 4, 5, 10, 25, 50, 100) ppb.

3.9. Optimization Procedures

In order to optimize the conditions for the OSW-ASV analysis using PANI-ZnO/GCE sensor and to obtain the greatest sensitivity and reproducibility for the determination of analytes, the influence of a number of analytical parameters such as pH concentration, deposition time, and deposition potential were carefully optimized in the first step of this experiment. The

dependence of the different anodic stripping peak current of the metal ions on the accumulation time in the standard solution was examined at constant concentration, pH, scan rate and deposition potential of the metal ions in different time range. Similarly, others parameters (deposition time, concentration, pH, scan rate) were optimized.The effect and dependence of the stripping peak signal of the metal ions under consideration on concentration was studied by varying the concentration within the range of 0 to 100 ppb of the standard solution keeping other parameters (deposition time, deposition potential, pH) being constant.

3.10. Voltammetric Detection Procedures

The voltammetric detection procedure consisted of pre-concentration (accumulation), cathodic electrolysis (deposition) and stripping (detection) steps. During preconcentration step, the electrode was immersed in a cell containing 10 mL of metal ion solution for a few minutes and stirred at 300 rpm. The electrode was then removed, rinsed with deionized distilled water and again immersed in to the voltammetric cell containing metal solution to be analyzed. A negative potential was applied to the electrode for few seconds. The stripping voltammetry was performed in the same cell by anodic stripping potential toward positive direction. Accurately measured 10 mL NaAC pH= 5.2 solution was measured and pipette in to a cell. Prior to the electrochemical measurements, the solutions were deoxygenated (the air present in the solutions were removed) by purging with argon gas for 5 minutes and then for accumulation the solution was stirred at speed of 300 rpm. After the accumulation (deposition) period, the stirring was stopped, and after 10 seconds of rest time, a deposition potential was applied for 30 to 240 seconds and then the metal deposited stripped by scanning into anodic (positive) direction. Stripping measurement was done under optimal instrumental parameters. The same procedure was applied for supportive electrolyte, samples and standard solutions. After all the measurements, peak current versus concentration which shows the amount of metals present in the solution were plotted.

3.11. Real Sample Preparations

Water samples taken in bottles (500 mL volume) from the four stations were transported to the laboratory and stored in refrigerator (±4^{o}C) until the measurements. To analyze the content of toxic heavy metals, 3 mL of conc. HNO_3 was added to each bottle. The beakers (50 mL) were cleaned and then 20 mL water samples collected from the four stations were appropriately added into the cleaned 50 mL beakers and then 2 mL of concentrated HNO_3 for acid digestion to minimize organic particles interferences prior to estimation of the toxic heavy metals. Therefore, acid digestion was done by mixing 20 mL of water sample with 2 mL of concentrated HNO_3. The beakers were heated at 80 ^{o}C for 2 h. After cooling the sample another 2 mL of concentrated HNO_3 were added. Each beaker was covered with watch glasses and returned to the hot plate again and the temperature was increased until a gentle refluxing action was occurred. Heating was continued by adding additional acid as necessary until digestion was completed which was indicated by a light colored residue. Furthermore, the beaker was warmed slightly to dissolve the residue by adding 2 mL of concentrated HNO_3.The wall of the beakers and watch glasses were washed down with deionized distilled water and the sample was filtered using Whatman No. 42 filter paper (Buffle *et al*., 2005). The final volume of the filtered water samples were adjusted to 50 mL with distilled water. The sample labelled and kept in refrigerator until the experimental determination of the toxic heavy metals (Chtaini *et al*., 2000b).

3.12. Application of PANI/ZnO/GCE as Electrochemical Sensors

To apply ZnO-PANI hybrid material as electrochemical sensor for the detection of Cd^{+2}, Pb^{+2}, As^{+3} and Hg^{+2}a three electrode arrangement will be set up in 10 mL electrochemical cell and the standard solution of (0, 0.1, 0.5, 1, 2, 3, 4, 5, 10, 25, 50, 100) ppb electrochemical response was measured using SWASV. The SWASV of electrodeposited metal ions will be performed in the potential range -1.3.0 to 0.5 V and detection of Cd^{+2}, Pb^{+2}, As^{+3} and Hg^{+2}have been performed at the experimental optimization condition. Then the unknown sample will be analyzed under similar condition.

4. RESULTS AND DISCUSSION

4.1. Structural and Morphological Characterization

4.1.1. Uv-vis Spectroscopy

Figure 7 shows those Uv–vis spectra of the ZnO nanoparticles dispersedin chloroform, the PANI and the PANI/ZnO nanocomposites dissolved in DMF. The absorption spectrum of the ZnO nanoparticles at 378 nm. It had shown two absorption bands characteristic of peak PANI at wavelengths 310 and 390 nm. The first absorption band arises from π-π^* electron transition within benzenoid segments. The second absorption bands are related to the formation of a quinoid segments (π polaron and π^* polaron) transitions, respectively. These results showed that PANI was completely converted from emeraldine salt to the emeraldine base form by the deprotonation of PANI. The absorption peak of PANI/ZnO occurred at 402 nm, which is red shifted compared with the absorption peaks of PANI (390 nm) and of ZnO nanoparticles (378 nm). This may be because of interactions between PANI chains and ZnO nanoparticles which cause easy charge transfer from PANI to ZnO via hydrogen bonding (Talwar *et al.,* 2014; Olad *et al.,* 2012).

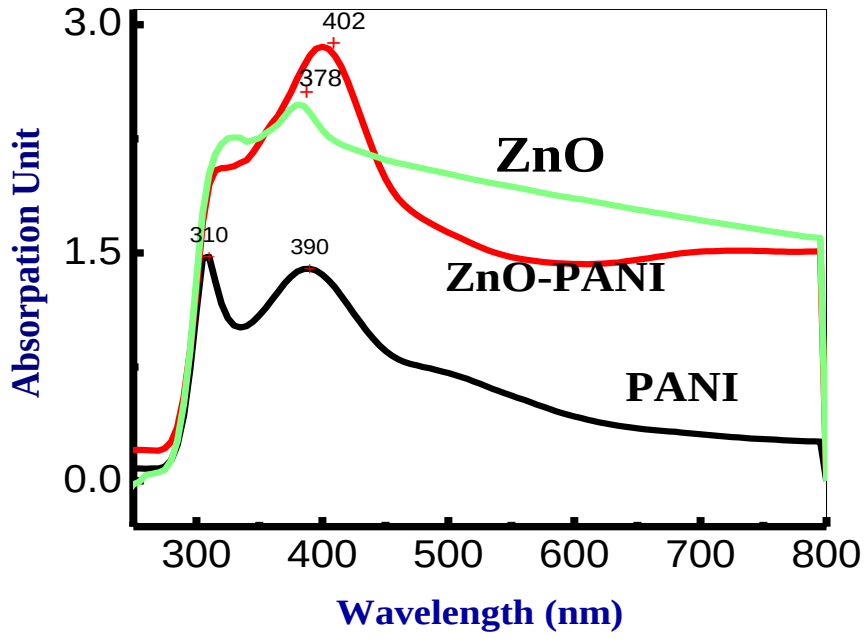

Figure 7. Uu-vis spectra of ZnO, PANI, and PANI/ZnO nanocomposites.

4.1.2. Fourier Transform Infrared (FT-IR) Spectroscopy

Fourier Transform Infrared (FT-IR) spectroscopy was employed to characterise the structures of the as synthesized ZnO, PANI and PANI/ZnO nanocomposites. FT-IR spectrum of ZnO nanoparticles shows significant absorption peaks at 3436, 2426, 1620, 1384, 836, and 434 cm^{-1} in (Figure 8a). The absorption band at 434 cm^{-1} was assigned to Zn-O stretching vibration (Xiong *et al.*, 2006). As seen in Figure 8b, the PANI exhibits characteristic peaks around 3448 cm^{-1} attributed to N–H stretching mode (Zheng *et al.*, 1997), the absorption peaks observed at 2924 and 2848 cm^{-1} are due to asymmetric C-H and symmetric C-H stretching vibrations (Gupta *et al.*, 2010), the peaks at 1569 and 1471 cm^{-1} correspond to C=C stretching mode for aromatic ring and the peaks at 1463 and 1113 cm^{-1} are assigned to C–C ring asymmetric and symmetric stretching vibrations of quinonoid and benzenoid rings, respectively. The presence of the benzenoid and quinoid units is evidence of the emeraldine form of PANI.

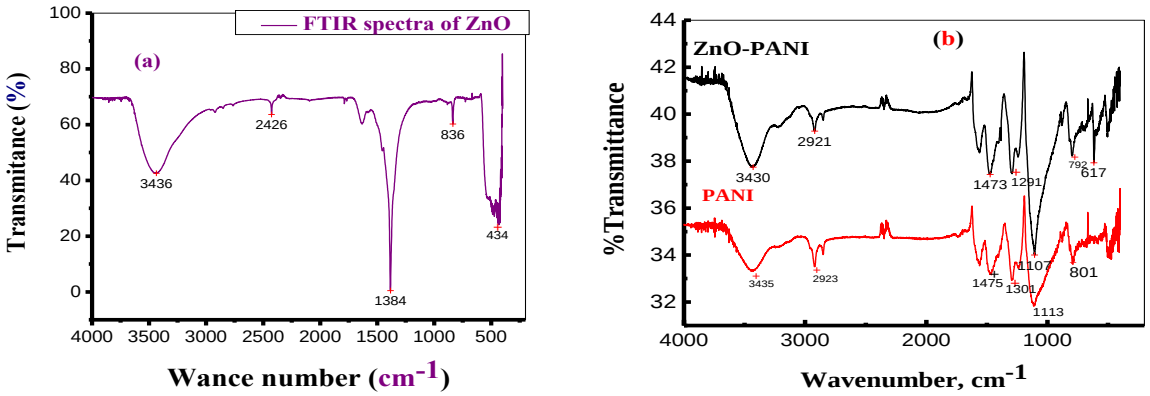

Figure 8. FT-IR spectra of (a) ZnO and (b) PANI and PANI/ZnO nanocomposites

The FTIR spectrum of the PANI/ZnO nanocomposite in Fig. 8b represents the same characteristic absorption peaks with the PANI nanoparticles. However, the corresponding peaks are shifted to the lower wave numbers, besides their intensities are changed after the addition ZnO nanoparticles. The peaks of the PANI around, 1301, 1113 and 801 cm^{-1} are shifted to 1291, 1105 and 792 cm^{-1}, respectively. These shifts of characteristic peaks of the PANI may be the result of the interactions between the PANI chains and ZnO nanoparticles which affect the electron densities and bond energies of the PANI (Niu *et al.*, 2003, Wang *et al.*, 2010). The shifting to the lower wave numbers may show the increasing the electron density of PANI chains.

4.1.3. Scanning Electron Micrographs (SEM) and EDX analysis

Figures 9(a–d) shows the HR-SEM images of bare (blank sample), ZnO, PANI nanoparticles and ZnO–PANI composite thin films, respectively. The SEM image of the pure PANI films (Figure 9c) exhibits a microsphere structure (Johnson, 2011). Figure 9(b) shows rod-like morphology of the ZnO. The SEM image of the composite thin films (Figure 9d) shows the agglomeration of ZnO nanoparticles engulfed in the PANI film. The EDX reveals that the required phase has present. carbon of PANI(C) is present in the sample. Again the graph shows the presence of O. This is due to the substrate over which it was held to do the SEM characterization.

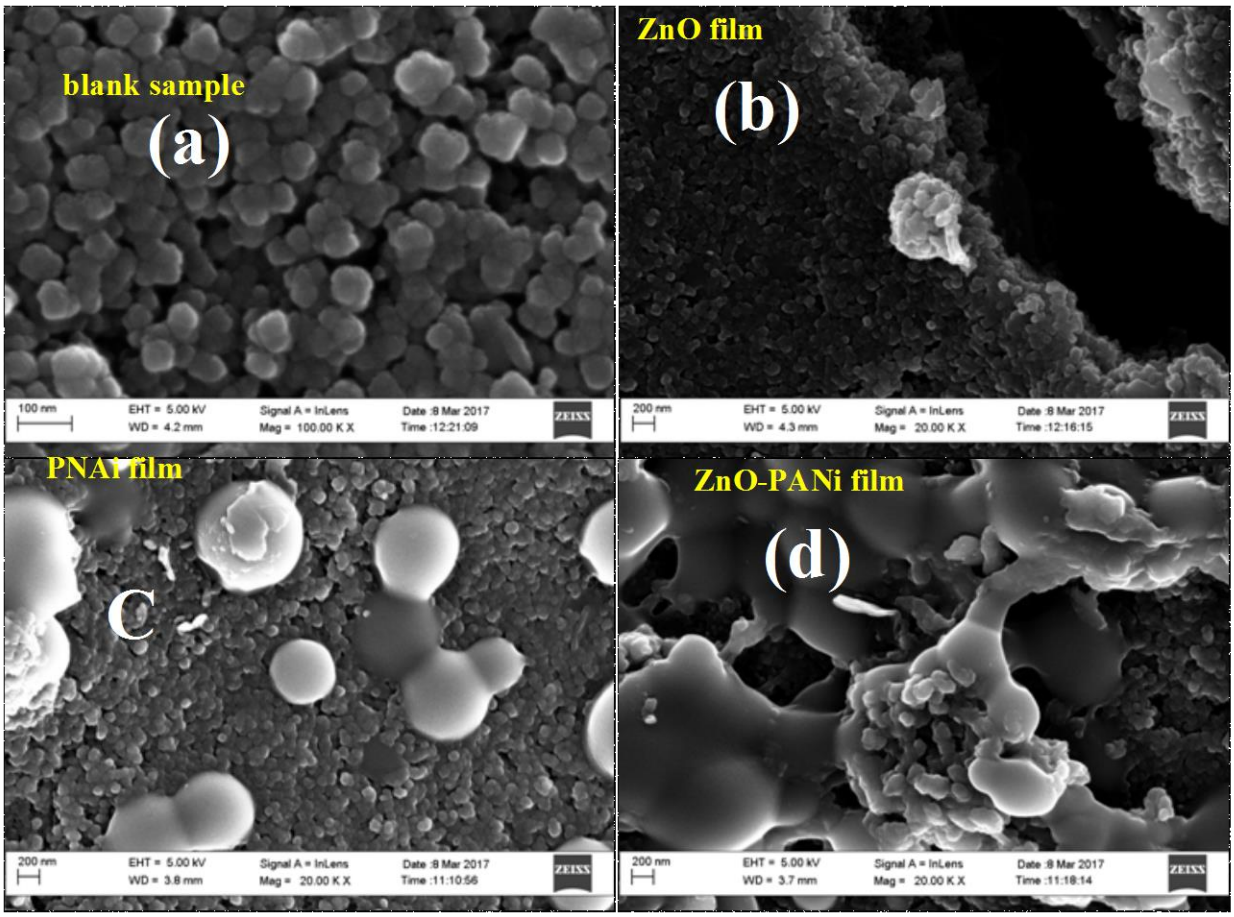

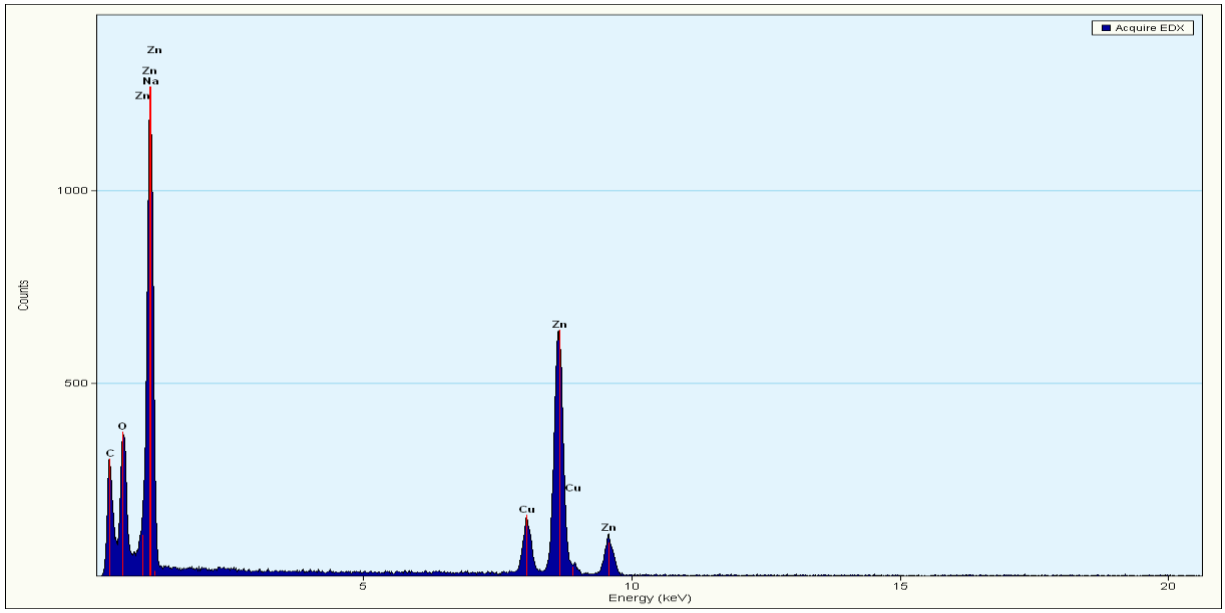

Figure 9. SEM images of (a) bare, (b) ZnO, (c) PANI and (d) PANI/ZnO NCs thin film and EDX analysis of ZnO-PANI

4.1.4. Transmission Electron Microscopy (HR-TEM)

Transmission electron microscope (HR-TEM) images (Figures 10(a-c) of ZnO, PANI and PANI/ZnO nanocomposite. Figure 10a shows the TEM micrograph of ZnO nanoparticles which are homogeneous and agglomerated. It is clear from the TEM micrograph that the particles are nearly spherical in shape. TEM image of PANI/ZnO nanocomposites as shown in Figure 10(c) clearly shows entrapping of ZnO nanoparticles in PANI matrix. Further more, the nanoparticles are homogeneous (Gupta *et al*., 2010; Niu *et al.*, 2003). The increase in the size of nanoparticles in the nanocomposites indicates that the surface of nanoparticles has interaction with PANI molecular chains, which is also supported by FT-IR analysis. The EDX analysis reveals that the required phase has present. Zn of ZnO, C of PANI(C) is present in a sample. Again the graph shows the presence of Cl and S. This is due to the substrate over which it was held to do the TEM characterization.

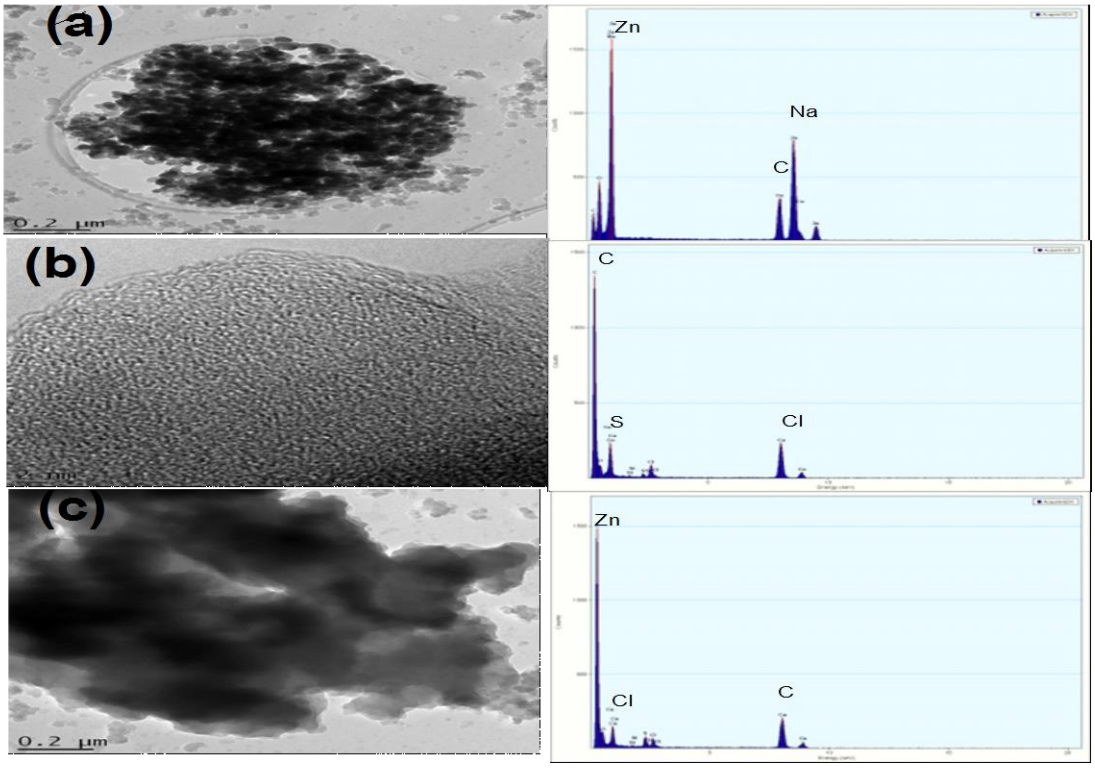

Figure 10. TEM image of (a) ZnO, (b) PANI, (c) PANI/ZnO NCs thin film & its EDX analysis

4.2. Cyclic Voltammograms of $K_3[Fe(CN)_6]$ on GCE

BAS100B electrochemical Bio-analyzer and Ag/AgCl (saturated 3 M KCl) reference electrode working status was tested using potassium ferrocynide 2 mM $K_3[Fe(CN)_6]$/1.0 M KCl solution which is a well-known model compound for reversible process. $K_3[Fe(CN)_6]$ was also used as a redox probe. Voltammetric behavior was studied both on bare electrodeand polyaniline-zinc oxide modified GC electrode. Cyclic voltammograms of 2 mM $K_3[Fe(CN)_6]$ in a potential range from -0.20 to 0.65 V is shown in(Figure 11).

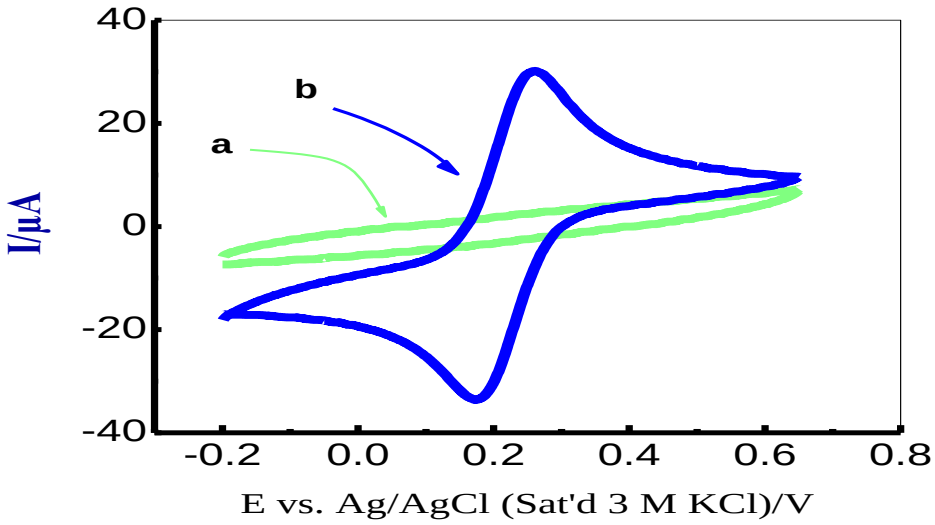

Figure 11. CV of supporting electrolyte 1.0 M KCl (a) and 2 mM $K_3[Fe(CN)_6]$/1 M KCl (b): at scan rate of 50 mVs^{-1}.

The effects of scan rate from 10 to 200 mVs^{-1}on peak potential were examined at different scan rates. As the scan rate increase the anodic and cathodic peak potential approximately remains constant. In addition to this the difference in anodic and cathodic potential falls in the range from 64−99 mV, which conforms the reversibility of $K_3[Fe(CN)_6]$ redox process on GCE with a slight deviation from its ideal value (60 mV) in (Appendix Table 7) (Roa *et al*., 2003; Beltagi *et al*., 2011). The redox potential of $K_3Fe(CN)_6$ was found to be 78, in agreement with litrature (Zhang *et al*., 2000).The redox peaks with the anodic and the cathodic peak potential appeared around 260 and at 172 mV vs. Ag/AgCl, respectively.

Anotherjustification for the reversibility of the process on GCE come from the ratio of peak current which was found to be nearly (Appendix Table 1).

4.3. Electropolymerization of Aniline on GCE and ZnO/GCE

Cyclic voltammograms recorded in the course of electropolymerization of aniline in 1.0 M HCl aqueous solution on GC electrode in a potential range from-0.6 to +1.1 V at scan rate of 50 mVs^{-1} are shown in (Figure 12a). The first cycle is characterized by an irreversible oxidation of aniline during the forward scan. When the potential is switched in the reverse scan three cathodic waves appeared. The origin of the anodic wave is attributed to the oxidation of aniline to its radical cation and the cathodic waves are as a result of the reduction of the polymer deposited at the electrode surface following the electro-generation of the radical cations or they have been explained to different redox state of PANI during polymerization step or the insertion of counter ions of the electrolyte into polymer matrix for charge balance following the change in oxidation state of the polymer upon reduction.

As read from the last polymerization cycle; the three anodic peaks appeared at about 282.2, 511.7 and 752.0 mV *vs.* Ag/AgCl and three cathodic peaks occurred at 71.9, 437.9 and 637.3 mV for the first, second, and third waves respectively (Figure 12a3). The three redox couples are associated with inter-conversion the first redox peak A/A$^{'}$ due to the conversion of leucoemeraldine to emeraldine salt while the third redox peak C/C’ is due to the conversion of emeraldine salt to pernigraniline form (Oluwakemi *et al.,* 2013).The redox couple B/B$^{'}$ at the centre is due to intermediates such as the benzoquinone and the hydroquinone in the polyaniline as it was reported in the literature (Dhand *et al.,* 2011; Morrin *et al.,* 2005). This pair of peaks (middle one) 511.7/437.9 mV may also indicate that, the presence of cross-linking of PANI caused by the reaction of species being present as intermediates products.

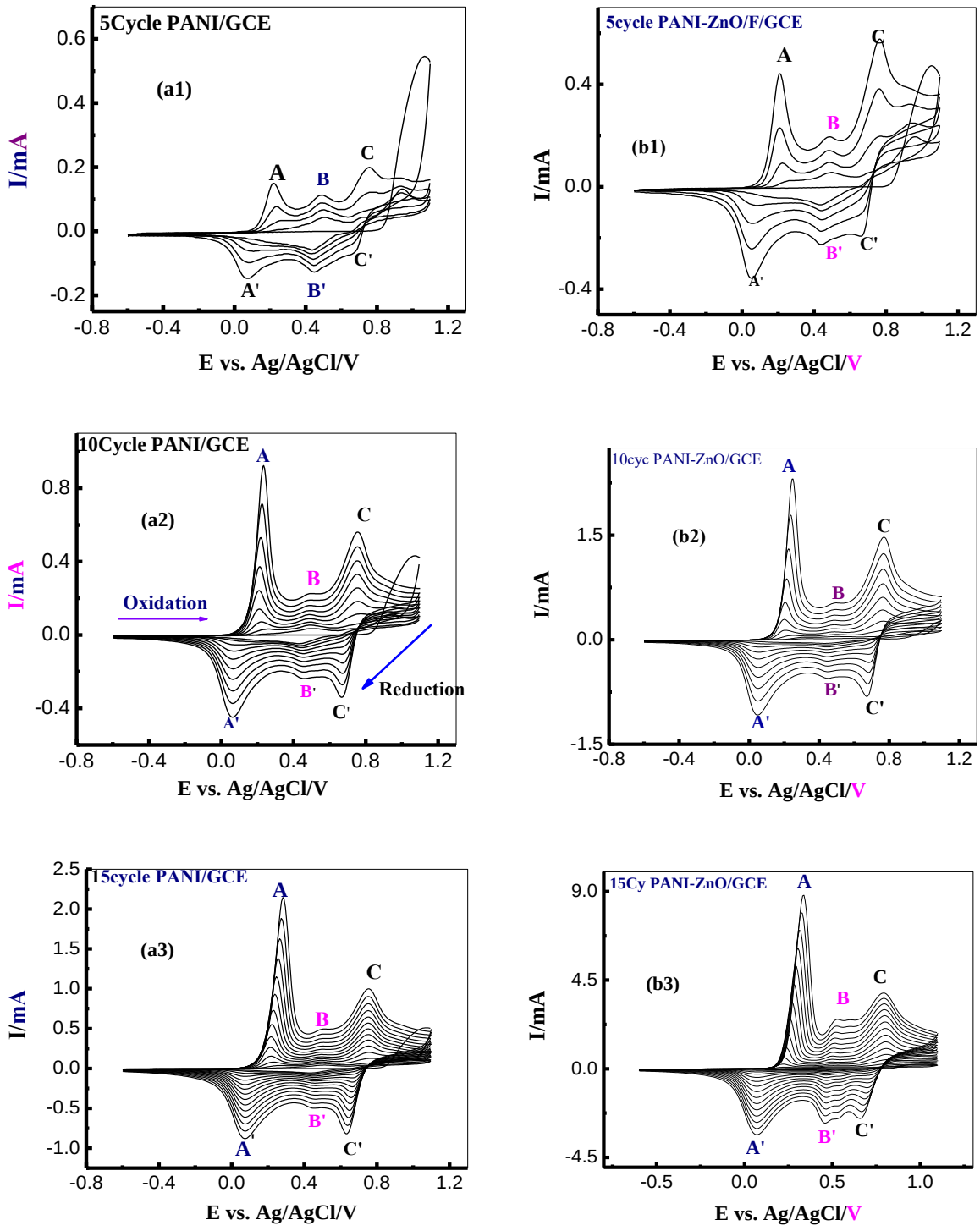

Figure 12. CV for the electrodeposition of PANI films at various thickness on GCE (a), ZnO/GCE (b) in 1.0 M HCl: potential window (-0.6 to +1.1 V) and scan rate = 50 mVs^{-1}.

In fact that anodic and cathodic peak potential difference of the first (210.3 mV) and the third (114.7 mV) are much greater than 60 mV vs. Ag/AgCl and these redox couples are irreversible. In contrast to this the second redox peak behaves a reversible process as indicated by its potential difference in the order of 73.8 mV and peak current ratio around unity. Besides, the peak ratio of the first redox couple is much higher than unity, which indicates that the film formed undergoes a follow-up reaction in the electropolymerization process (Figure 12a3) (Arjomandi and Tadayyonfar, 2013).

On the other hand, similar to PANI grown On GC three anodic 339.6, 525.3 and 787.6 and three Cathodic 71.9, 465.3 and 659.2 mV formed during the electropolymerization of PANI on ZnO modified GC electrode (Figure 12b3). The rate of polymerization of PANI seems faster on the modified electrode. This was informed based on the fact that the anodic polymer growth current (i_{ox}) of the last growth cycle of the first and third peak during all polymerization cycles in the case of PANI/ZnO/GC ($i_{ox,A}$ = 8.81 mA, $i_{ox,C}$ = 3.86 mA) was higher than that of PANI/GC ($i_{ox,A,}$ = 2.14 mA $i_{ox,C}$ = 1.0 mA,) (Table 4). The peak oxidation current of PANI/ZnO/GC was the largest this is because ZnO increase the surface area and it has catalytic behavior.

Comparison of Figure12 (a3 and b3) indicates that PANI characterized with a larger apparent peak current on ZnO/GC electrode than GCE. PANI film deposited on ZnO/GC was found to be the most electroactive when comparing peak to charge per peak per unit concentration based on the CV at 50 mVs^{-1} (Table 3 and 4) followed by PANI/GCE. This could be either due to large mass of polymer deposited or increased surface concentration.

Table 3. Electrochemical polymerization parameters of PANI/GCE in 1.0 M HCl(aq)

PANI/GCE	Redox Couple	Ep_a/mV	Ip_a/A	Epc/ mV	Ip_c/A	Ipa/Ipc	ΔE (mV)	$E^{0'}$ (Mv)
5cycle	A/A'	219.4	$1.505E^{-4}$	77.4	$-1.467E^{-4}$	1.0	142.0	148.4
	B/B'	478.9	$1.126E^{-4}$	443.4	$-1.277e^{-4}$	0.9	35.5	461.15
	C/C'	754.8	$1.995e^{-4}$	672.8	$-6.767e^{-5}$	2.9	82.0	713.8
10 cycle	A/A'	235.8	$9.233e^{-4}$	61.0	-4.220^{e-4}	2.2	174.8	148.4
	B/B'	489.8	$2.277e^{-4}$	457.1	-2.427^{e-4}	0.9	32.7	473.45
	C/C'	757.5	$5.597e^{-4}$	667.4	$-3.415e^{-4}$	1.6	90.1	712.45
15 cycle	A/A'	282.2	$2.144e^{-3}$	71.9	$-8.838e^{-4}$	2.4	210.3	177.05
	B/B'	511.7	$5.075e^{-4}$	437.9	$-5.043e^{-4}$	1.0	73.8	474.8
	C/C'	752.0	$9.976e^{-4}$	637.3	$-8.285e^{-4}$	1.2	114.7	694.95

Table 4. Electrochemical polymerization parameters of PANI/ZnO/GCE in 1.0 M HCl(aq)

PANI-ZnO/GCE	Redox Couple	Ep_a/mV	Ip_a/A	Epc/ mV	Ip_c/A	Ipa/Ipc	ΔE (mV)	$E^{0'}$ (Mv)
5cycle	A/A'	211.2	4.379e-4	52.8	-3.585e-4	1.2	158.4	132
	B/B'	492.6	1.949e-4	432.5	-2.261e-4	0.9	60.1	462.55
	C/C'	765.7	5.763e-4	667.4	-1.945e-4	3.0	98.3	716.55
10 cycle	A/A'	249.5	2.313e-3	52.8	-1.086e-3	2.1	196.7	151.15
	B/B'	498.0	5.265e-4	437.9	-5.407e-4	1.0	60.1	467.95
	C/C'	768.4	1.475e-3	670.1	-8.016e-4	1.8	98.3	719.25
15 cycle	A/A'	339.6	8.810e-3	71.9	-3.374e-3	2.6	267.7	205.75
	B/B'	525.3	2.555e-3	465.3	-2.751e-3	0.93	60	495.3
	C/C'	787.6	3.860e-3	659.2	-2.573e-3	1.5	128.4	723.4

4.4. Effects of Film Thickness of PANI on GCE and ZnO/GCE

There are two ways to increase the amount of PANI coating during electropolymerization. These are a higher aniline monomer concentration in a solution and a longer polymerization

time. In this work, polymerization time was increased by increasing the number of scan cycles during the cyclic voltammetric deposition. The voltammograms measured during the synthesis of the PANI coatings on the GCEand ZnO/GCE in theelectrolyte of 1.0 M HCl containing 0.1 M aniline monomers using CV method are shown in Figure 12a and 12b, respectively.

The oxidation peaks at about 0.334 V are related to the transformation of the deposited PANI coatings from leucoemeraldine form (fully reduced state) to emeraldine salt (neutral state). The oxidation peaks at about 0.525 V refer to the state transformation from emeraldine to pernigraniline (fully oxidized state) Figure 12b3. The oxidation peaks at about 0.788 V are related to the polymerization reactions of aniline. As the number of scan cycles increases, the two main peaks increase, which indicates that thicker PANI coatings have been formed. Thus, the PANI coatings can be used to modify the GCE for the application of anodic stripping voltammetric determination of trace heavy metals. The PANI coatings have a porous and branched structure that can increase the specific surface area.

As the number of scan cycles increases from 5 up to 15 cycles, the coatings get thicker and more uniform, and at the same time, the color of the coatingchanged from light green to dark green that remains unchanged even after a few days of exposure to air. At the film-solution interfaces the charge transfer resistance of the PANI coatings is affected by the thickness, specific surface area, conductivity, doping level, and oxidation state of the coatings. A longer deposition time can lead to a thicker PANI coating with a reduced density of porosities, which results in a higher charge transfer resistance (Wang *et al.*, 2011).

As the number of cycles increased, the first anodic peak potential becomes more positive and third peak becomes more negative which probably due to possibly conjugation length increase with successive cycles (Genies and Tsintavis, 2002). Up on scanning repetitively, the increase of anodic and cathodic currents confirmed the growth of the polymer film. Black green polymer film well adhered to the electrode surface was successfully formed on the polished GCE.

4.5. Electrochemical Characterisation of PANI and PANI/ZnO Films on GC

The electrodeposited ofPANI on GC and ZnO/GC electrodeswas characterized with cyclic voltammetry (10 to 100) mVs^{-1} in a fresh monomer free 1.0 M HCl solution. Both PANI and the nanocomposite polymer film were found to be electroactive. They exhibited two oxidation peak (E_{pa}^{A} = 322.7 mV, E_{pa}^{B} = 585.5 mV) and two reduction peaks ($E_{pa}^{A'}$ = 106.5mV, $E_{pa}^{B'}$ = 558.9mV) as shown in (Figure 13a3) on GC electrode and two oxidation (E_{pa}^{A} = 360.6 mV, E_{pa}^{B} = 577.8 mV) and two reduction peaks ($E_{pa}^{A'}$ = 127.2 mV, $E_{pa}^{B'}$ = 483.1 mV) on ZnO/GC electrode as shown in (Figure 13b3) and (Table 9). All the peak potentials indicated here are at scan rate of 50 mVs^{-1}.

Figure 13 (a3 & b3) shows the cyclic voltammograms of PANI on bare and ZnO/GCE respectively registered at different scan rates (5 to 100 mVs^{-1} in monomer free 1.0 M HCl(aq)). In contrast to polymerization in all cases two anodic and cathodic peaks observed specially at high scan rates. As the scan rate increases the oxidation peak potential shifts to more positive value which is a typically characteristics of movement of ions in and out of films and it indicating that both potentials (Ep_a, Ep_c) are functions of scan rates.

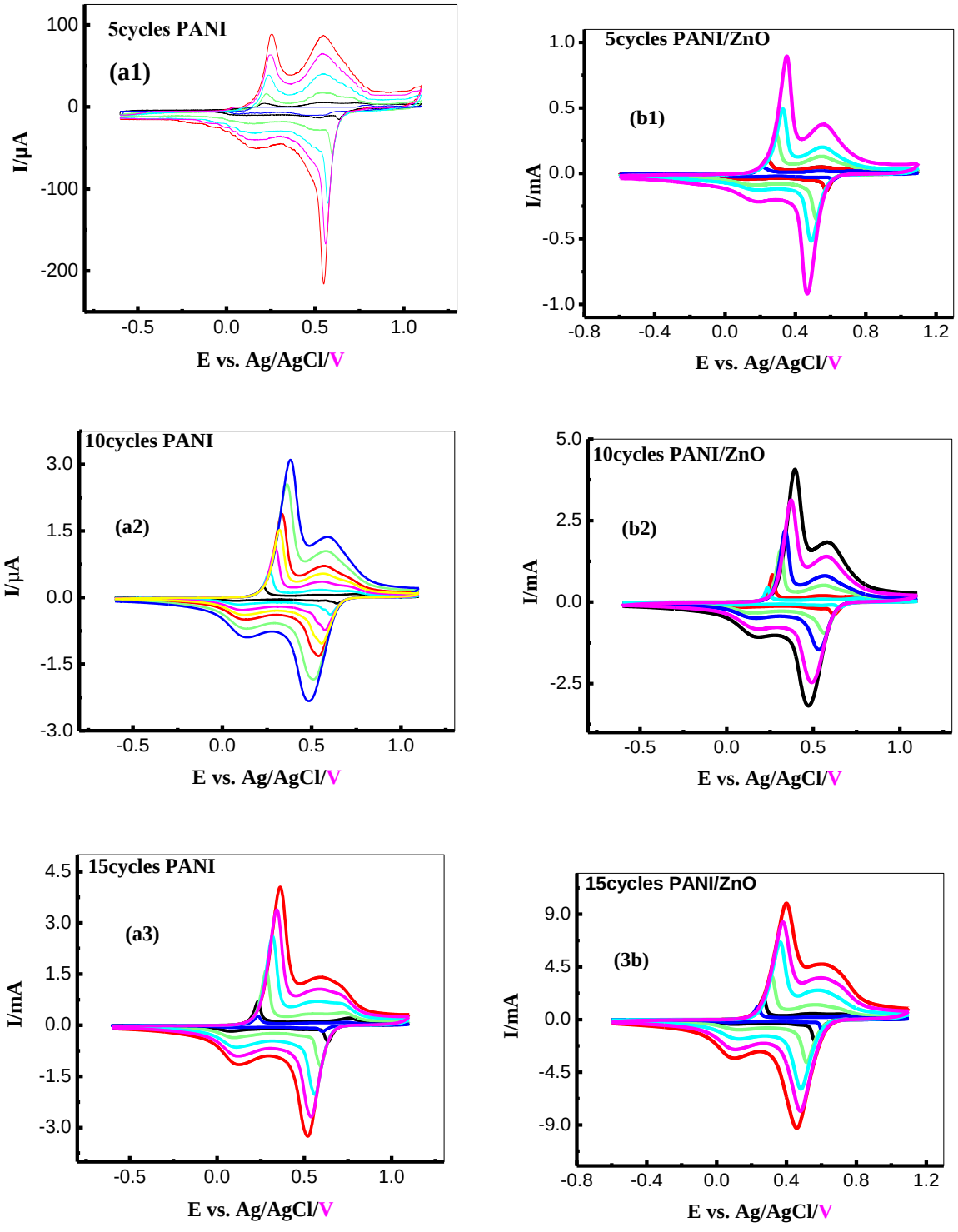

Figure 13. CV of electrochemically modified GCE characterization (a1 – a3) PANI (b1 – b3) PANI/ZnO filmon GCE at different scan rate (5, 10, 25, 50, 75 and 100) mVs^{-1}.

Figure 14a reveals that the anodic peak current is linearly proportional to the square root of scan rate, indicating a diffusion-controlled redox process. From the anodic peak current versus the square root of the scan rate slope, a linear dependence PANI/ZnO/GC electrode more reveals diffusion control by having the small peak to peak separation and linear regression (R^2 = 0.99931) than PANI/GCE. Therefore, the diffusion of H^+ ion in PANI/ZnO/GCE matrix was controlled (Juanjuan *et al*., 2008).

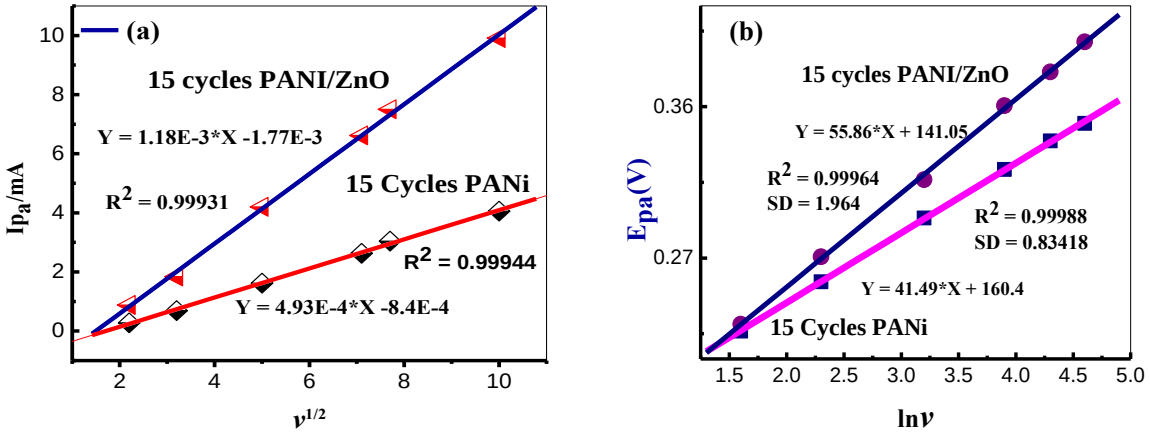

Figure14. CVof I_{pa} vs. $V^{1/2}$ (a) and E_{pa} vs. lnv (b) electrochemically characterized of 15 cycles of PANI/GCE and PANI-ZnO/GCE in 1 M HCl at scan rate (5, 10, 25, 50, 75 & 100) mVs^{-1}

In addition, the relationship between oxidation peak potential (E_{pa}) and natural logarithm of scan rate (ln*v*) is also shown in (figure 14b) it can be seen that plotting of the E_{pa} *vs.* ln*v* of PANI/GCE and PANI/ZnO/GCE produce a straight line at with equation and linear regression (0. 99988) and (0. 99964), respectively, shown in (Table 5) by using the redox peak.

The electron transfer rate constant k_s can be estimated by the **Laviron equation**:

$$E_{pa} = E^{o'} + \frac{RT}{\alpha nF} + \frac{RT}{\alpha nF} \ln\nu$$

$$\ln k_s = \alpha\ln(1-\alpha) + (1-\alpha)\ln\alpha - \ln\left(\frac{RT}{nF\nu}\right) - \alpha(1-\alpha)\left(\frac{nF\Delta E}{RT}\right)$$

The nα value can be calculated for each electrode by using the slope of E_{pa} *vs.* ln*v* plot.

$$\frac{RT}{\alpha nF} = \text{Slope}$$

The PANI-ZnO/GCE produced electrode has lower peak to peak separation than others. Small peak-to-peak separation always indicates a fast electron transfer rate (Liu *et al*., 2008). The electron transfer rate constant k_s are estimated to be $0.1667s^{-1}$ from this formula, which is much larger than that of PANI ($0.123s^{-1}$). Therefore, the PANI/ZnO nanocomposites can provide excellent facilitate the electron transfer reaction.

Table 5. Kinetic parameters of PANI and PANI/ZnO electrodes

Electrode	Equation	α	k_s (s^{-1})
PANI/GCE	E_{pa} =55.86ln$v$ + 56.1, R = 0.99988	0.724	0.123
PANI/ZnO/GCE	E_{pa}=41.49ln$v$ + 44.57, R = 0.99964	0.658	0.1667

4.6. EC Characterisation of Chemically Synthesized PANI andPANI/ZnO

Polyaniline and PANI/ZnO nanocomposites produced chemically by in−situ oxidation polymerization method, their electrochemical properties were characterized employing cyclic voltammetry. This nanomaterials sonicated in DMF was drop coated to modify the GCE. Experimental parameterizes (potential range -0.6 to +1.1 mV, scan rate from 3 to 75 mVs^{-1} and 1.0 M HCl(aq) medium was similar to electrochemically produced once (Figure 12).

Voltammograms recorded during chemical polymerizations were indicated in (Figure 15). It is very clear that PANI is electro-active in 1.0 M HCl and showed two anodic and two cathodic peaks (Figure 13a) as observed from electrochemically formed film. The oxidation potential of PANI (E_a^A= 329.4 & E_a^B = 618.8mV) occurred silently at more negative value and as expected peak potentials of the mixture shift to more positive value as the scan rate increases (Figure 15b). In contrast to the electrochemically synthesized polymer film the first redox pear become a quasirreversible.

On the other hand, PANI/ZnO nanocomposites exhibits two oxidation and two reduction peaks at all scan rates.Two separate redox peaks correspond to two redox processes of PANI normally found in acid conditions, i.e., transition between fully reduced leucoemeraldine state (LM) and half-oxidized emeraldine state (EM), and transition between EM state and fully oxidized pernigraniline state (PE).

Table 6 show the anodic and cathodic peak potentials, peak potential differences between two redox couple of PANI and PANI/ZnOnanocomposites and their peak current ratio from (Figure15a-b). In contrast to the electrochemical synthesized, the voltammograms of PANI and polymer nanocomposites materials (Figure 13a and b)at 50 mVs^{-1} depicts PANI are less electroactive compare to and PANI/ZnO. This may be the presence of ZnO amount in the composite and highly incorporation of ZnO nanoparticles in polyaniline films which may create a good catalytic activity to free movement of ions (Figure 15b) and (Table 6).

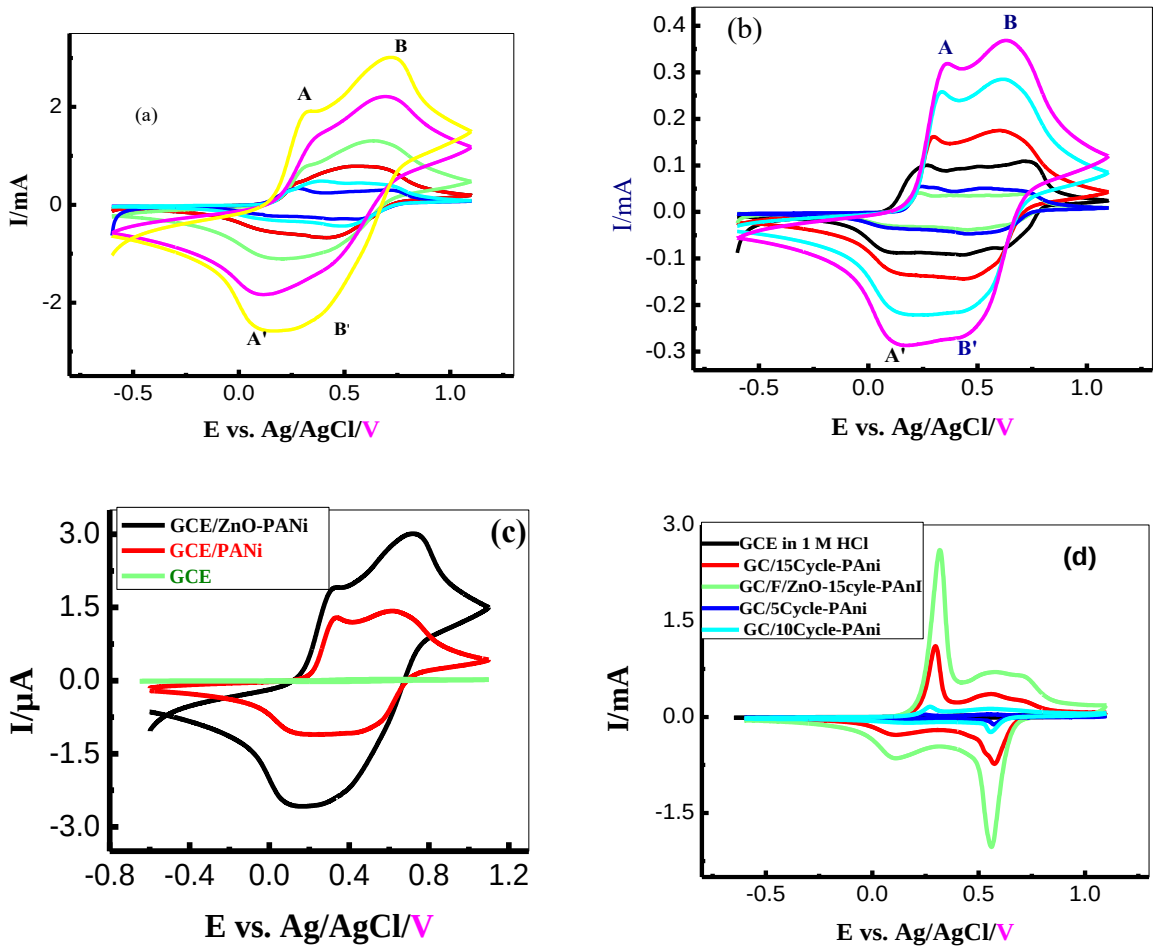

Figure 15. CV of chemically synthesized PANI (a) PANI/ZnO (b) films on GCE, characterizat ion in 1 M HCl: potential window = -0.6 to +1.1 V; at different scan rate (3, 5, 10, 25, 50 and 75) mVs^{-1} and (c and d) are the overlay of the CV's of GCE, PANI/GCE and PANI-ZnO/GCE performed in 1 M HCl at scan rate: 50 mV s^{-1} & 1 mA/V.

Table 6. Parameters of chemically modified GC electrode in 1M HCl at 50mVs^{-1}.

Electrodes	Redox	E_{pa}(mV)	E_{pc}(mV)	I_{pa}(mA)	I_{pc}(mA)	I_{pa}/I_{pc}	ΔE
PANI	A/A’	329.4	157.9	1.3	1.4	0.9	243.6
	B/B’	618.8	458.9	1.1	1.1	1.0	538.8
PANI/ZnO	A/A’	374.1	106.7	1.9	3.0	0.6	240.4
	B/B’	718.6	403.7	2.5	2.2	1.1	561.1

From electrochemical characterization of both chemically and electrochemically synthesized electrodes, figure 14 and 16 reveal that they have two redox peaks at scan 75 and 100mVs^{-1} and three redox peaks for lower scan rate 10, 25 and 50 mVs^{-1}. The synthesized electrodes in both method showed excellent polymerization of aniline with two separate redox peaks correspond to two redox processes of PANI normally found in acid conditions, i.e., transition between fully reduced leucoemeraldine state (LM) and half-oxidized emeraldine state (EM), and transition between EM state and fully oxidized pernigraniline state (PE). Figure 15c showed that the similarities of both method synthesized electrodes. When the surface increased the peak to peak separation is decreased in both cases, which indicates a good electron transfer reaction.

4.7. Electrochemical Impedance Spectroscopyof PANI and PANI/ZnO

Electrochemical Impedance Spectroscopy (EIS) were used to investigate the performance of the modified electrodes being an effective method of probing the features of a surface modified electrode. The measurement was performed in 1.0 M HCl aqueous solution with a frequency range of 100 kHz to 0.1 Hz of which the amplitude of the alternative voltage was 10 mV, as shown in Figure 16. The y-axis represents the negative number of the imaginary part of the measured impedance while the x-axis represents the real part of the measured impedance.

For a reaction that is reversible, the Nyquist plot usually exhibits two regions: (i) a semicircle at a high frequency region which corresponds to electron charge transfer process from which the electron-transfer resistance value can be measured directly, and (ii) a straight line section at low frequency region of the plot, which represents the diffusion-limited transport of the

redox species from the electrolyte to the electrode interface. After the modification of GCE with PANI film, the Rct value was reduced as was also the case with when GCE was modified with PANI/ZnO. The modified electrodes exhibited large semicircles and straight lines in the lower frequency region, indicating a sign of modification and charge transfer resistance but high diffusion system.

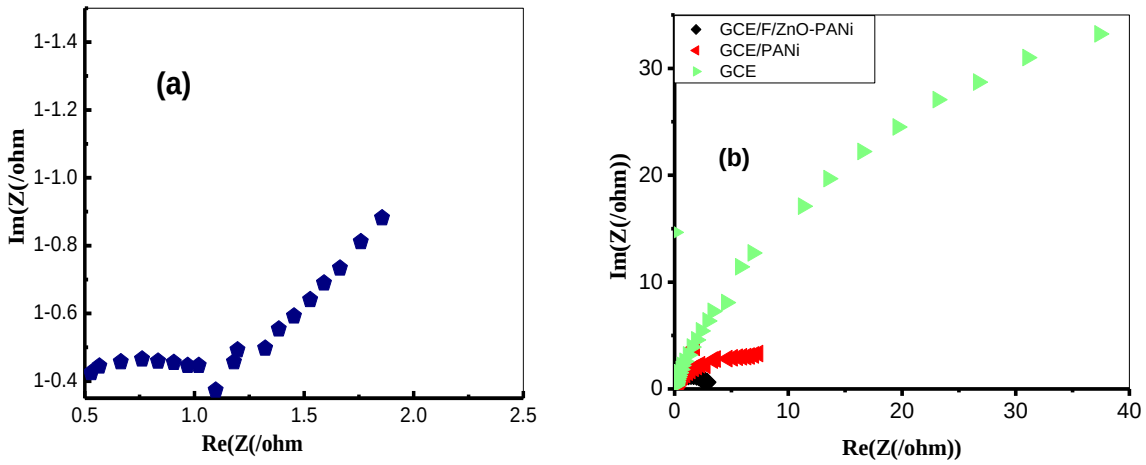

Figure 16. Nyquist plots of the EIS measurement of GCE, PANI and PANI/ZnO in 1 M HCl

4.8. Optimization Parameters of of PANI-ZnO/GCE Electrochemical Sensor

Voltammetry experiments were performed in two step measurements. In the first step, the metal ion present in the test solution was deposited on the surface of PANI-ZnO/GCE at their deposition potential and in the second step all the deposited ions were anodically stripped by scanning the potential for each metal. In the deposition process, stirring the solution can improve the accumulation efficiency. In stripping methods, only species that were in a labile form can be electrodeposited on PANI-ZnO/GCE and yield an analytical response owing to the anodic oxidation step. The mechanism for metal binding (accumulation) at PANi-ZnO/GCE surface is:

$(M^{n+})_{soln} + (PANi\text{-}ZnO/GCE)_{surface} \rightarrow (M^{n+}\text{-}PANi\text{-}ZnO/GCE)_{adsorb}$ (accumulation step)

$(M^{n+}\text{-}PANi\text{-}ZnO/GCE)_{adsorb} + ne^{-} \rightarrow (M^{o}, M\text{-}PANi\text{-}ZnO/GCE)_{adsorb}$ (reduction step)

$(M^{o}, M\text{-}PANi\text{-}ZnO/GCE)_{adsorb} - ne^{-} \rightarrow (M^{n+})_{sol}^{n} + (MPANi\text{-}ZnO/GCE)_{surface}$(stripping step)

In order to optimize the conditions for the (OSW-ASV) analysis and to obtain the greatest sensitivity and reproducibility for the determination of Cd, Pb, As and Hg, the influence of a number of analytical parameters such as pH, concentration, deposition time and deposition potential were carefully optimized in the first step of this experiment.

4.8.1. Optimization of pH

The pH value of a sample solution is one of the most important variables controlling the adsorption of the metal ions on the electrode. For selecting the solution pH, the stripping sensitivity of each element and the buffer capability were in consideration. The influence of the pH on the anodic stripping peak currents of Cd and Pb was studied whilst measuring the pH in the Voltammetric cell a solution containing 0.1 M sodium acetate buffer using HNO_3 and NaOH for pH adjustment in acidic and basic medium, respectively.

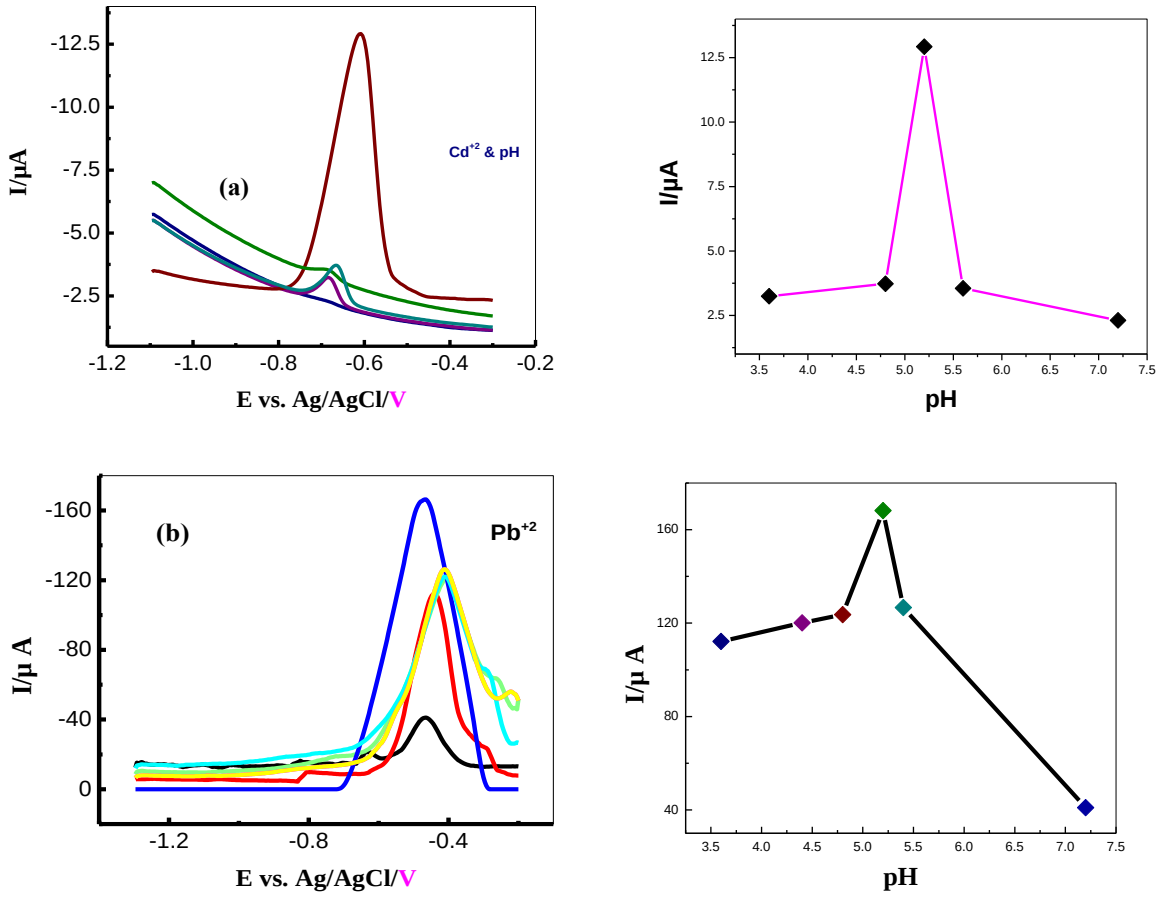

Figure 17. OSW-ASV a) Cd and b) Pb at different pH & at constant at scan rate of 60 mVs^{-1}, concentration 50 ppb and deposition time 90 sec.

As shown in (Figure 17), the stripping peak currents of the both metals increase as the pH increases from 3.6 to 5.2. However, when the pH is higher than 5.2, the both peak currents were dropped. The PANI coatings have increased conductivities due to higher concentrated H^+ doping at lower pH values, which may tend to increase the peak currents. However, the PANI coatings more positively charged can repulse the metal ions that are also positively charged due to higher concentrated H^+ doping at lower pH values (Zhaomeng *et al.*, 2011). In addition, the hydrogen evolution at a lower pH can be much easier, which can reduce the electrode surface activities. Because of the above two effects, the peak currents of the PANI-ZnO/GCE the peak signal increases from 3.6 to 5.2 and become sharp at pH of 5.2 and a maximum accumulation of these metal ions on the PANI-ZnO surface occurs at pH of 5.2.

Therefore, a well defined, sensitive and adequate value of anodic stripping peak current with best conditions was pH 5.2 taken to be the optimum conditioning for the quantifying of metal ions (Cd, Pb, As and Hg) and hence adapted for all subsequent experiments.

4.8.2. Optimization of Pre-Concentration Time

The dependence of the different anodic stripping peak current of the metal ions on the accumulation time in the standard solution was examined at constant concentration, pH, scan rate and deposition potential of the metal ions in the range of 30 to 300 seconds as shown in (Figures 18). As expected for anodic stripping experiment the peak current was increased with accumulation time but only up to 90 seconds. At longer deposition time than 90 seconds the stripping signals for metal ions become gradually decreases or had reached to the range of trace metal analysis level at this preconcentration time.

Therefore, the metal ions Cd and Pb were rapidly adsorbed on the PANI-ZnO/GCE surface at a deposition time of 90 secondswhile further prolonged accumulation time did not improve the peak height and the peak currents tend to level off slowly. Hence the ideal deposition time for the determination of these metal ions was selected to be 90 seconds and all the subsequent experiments were performed with in this accumulation time.

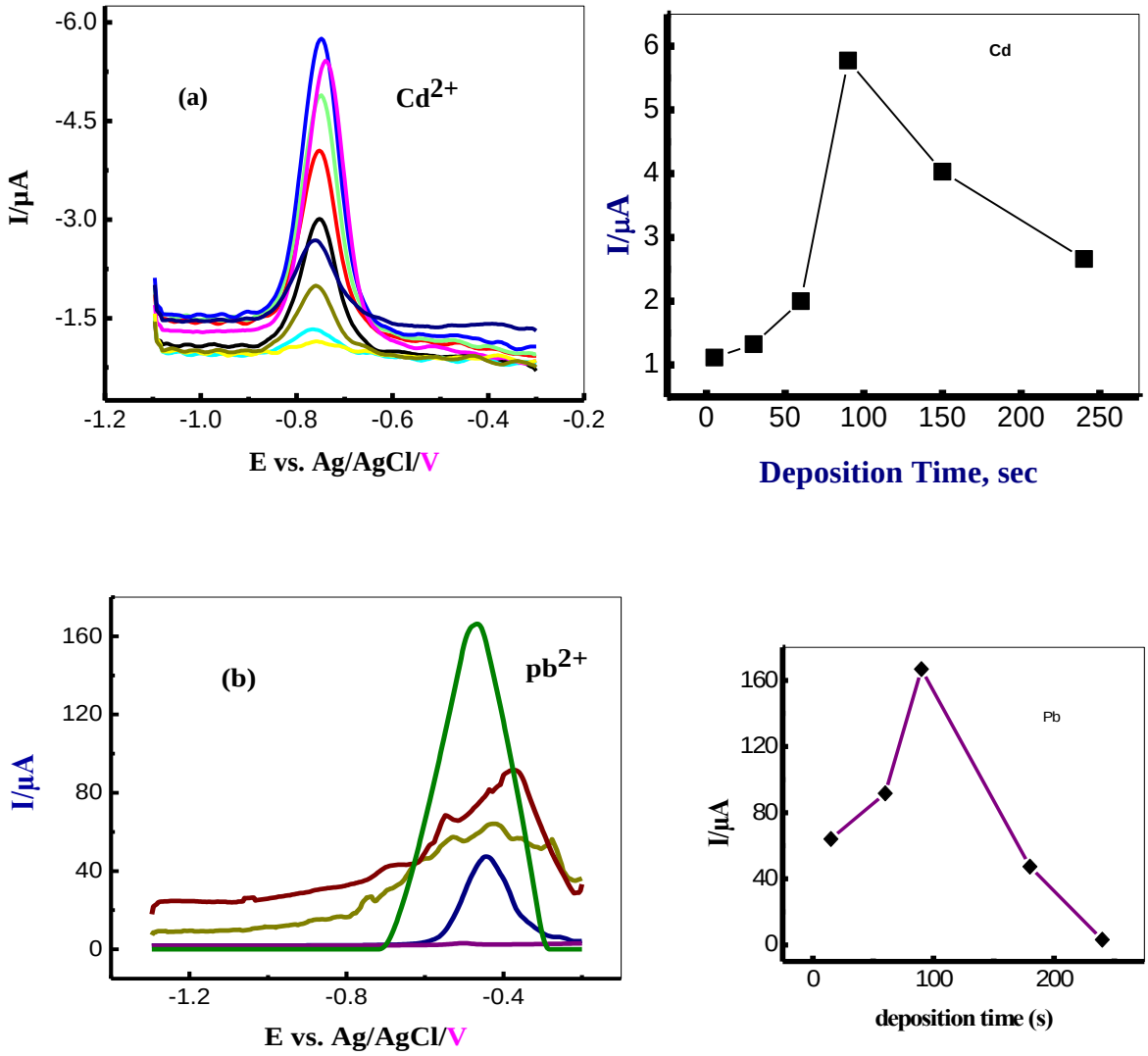

Figure 18. OSW-ASV a), Cd and b) Pb at d/t deposition time and at pH 5.2 NaACbufferand conc. 50 ppb. The inset plot shows the Plot of I_P vs. deposition time of a) Cd and b) Pb

4.8.3. Optimization of Pre-Concentration Potential

The influence of the variation of the accumulation potential on the peak current was studied and examined over the range of -1.3 to -0.3 Vand -1.1 to 0.0 V for Cd and Pb, respectively and fixed for each metal ion in the standard solution. While the peak current was almost constant at the deposition potential of these metal ions, with a slight increase or decrease in accumulation potential, the peak current was increased substantially with more negative

deposition potential and then the largest peak current started decreasing again at more positive potential. As it was seen from the experimental work (Figure 19), the accumulation potential for Cd and Pb, respectively has better sensitivity at a potential of -1.1 V and -1.3 V, respectively, and these accumulation potential (scanned at positive direction) was selected and applied to the later analytical measurements as the optimum condition for the determination of the identified metal ions.

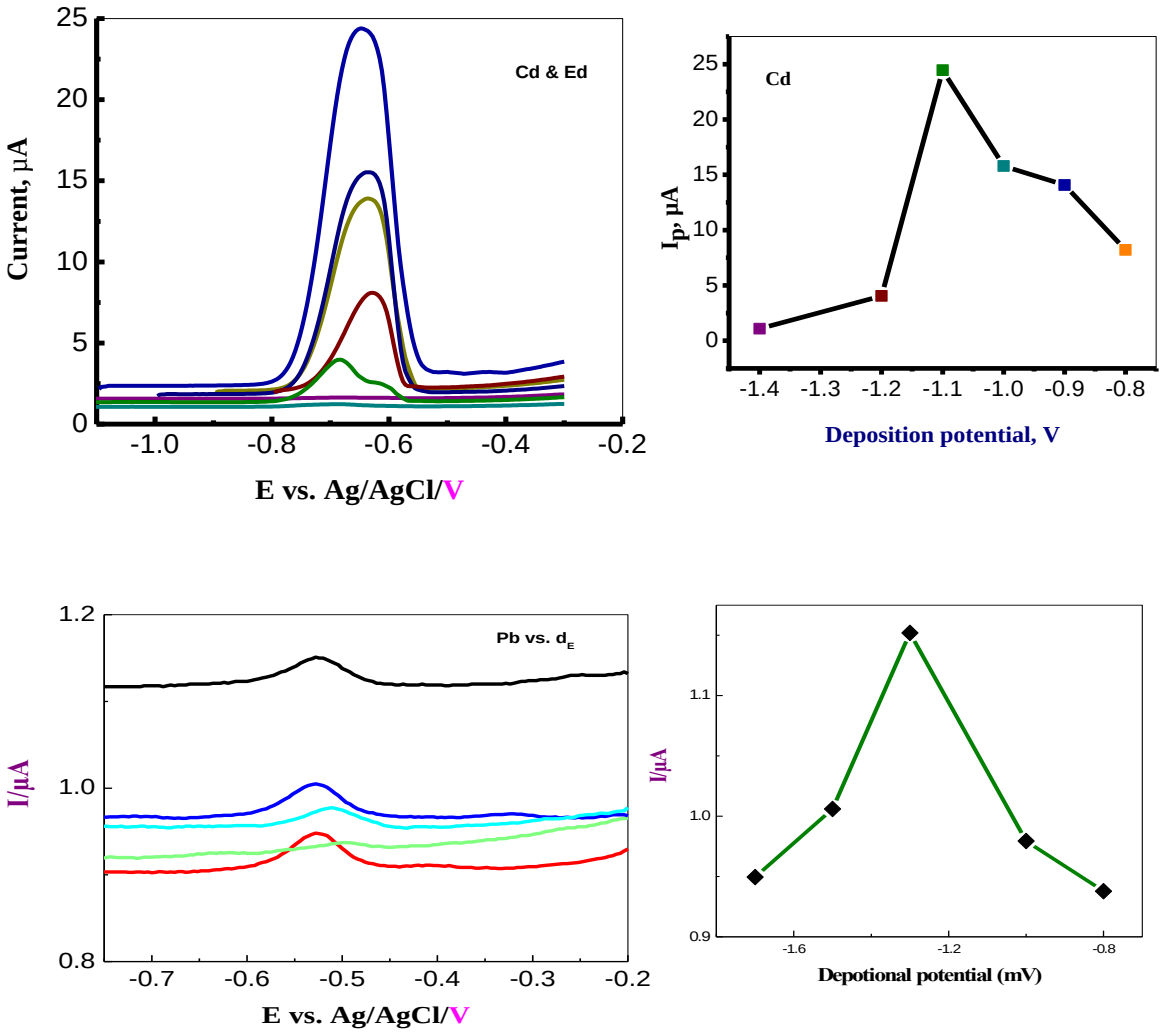

Figure 19. OSW-ASV of a) Cd b) Pb at different deposition potential and at pH 5.2 NaAa buffer, conc 50 ppb and deposition time 90 sec. The inset Plot shows the Plot of I_p versus deposition potential a) Cd and b) Pb.

4.8.4. Influence of the Variation of Concentration and calibration curve plot

The effect and dependence of the stripping peak signal of the metal ions under consideration on concentration was studied by varying the concentration within the range of 0 to 50 ppb of the standard solution keeping other parameters being constant as shown in Figure 20. At the standard concentrations of (0, 1, 5, 10, 20, 30, 50 and 100) ppb, the peak current of metals increased with increasing concentrations and there was a little change in the peak current beyond 100 ppb that is the peak current becomes broad. The electrode surface gets saturated early for higher concentration compared to the low concentration. Beyond 100 ppb, the peak current obtained was more intense, however, the signal was very broad and reproducibility was poor but the peak was sharp at 100 ppb.

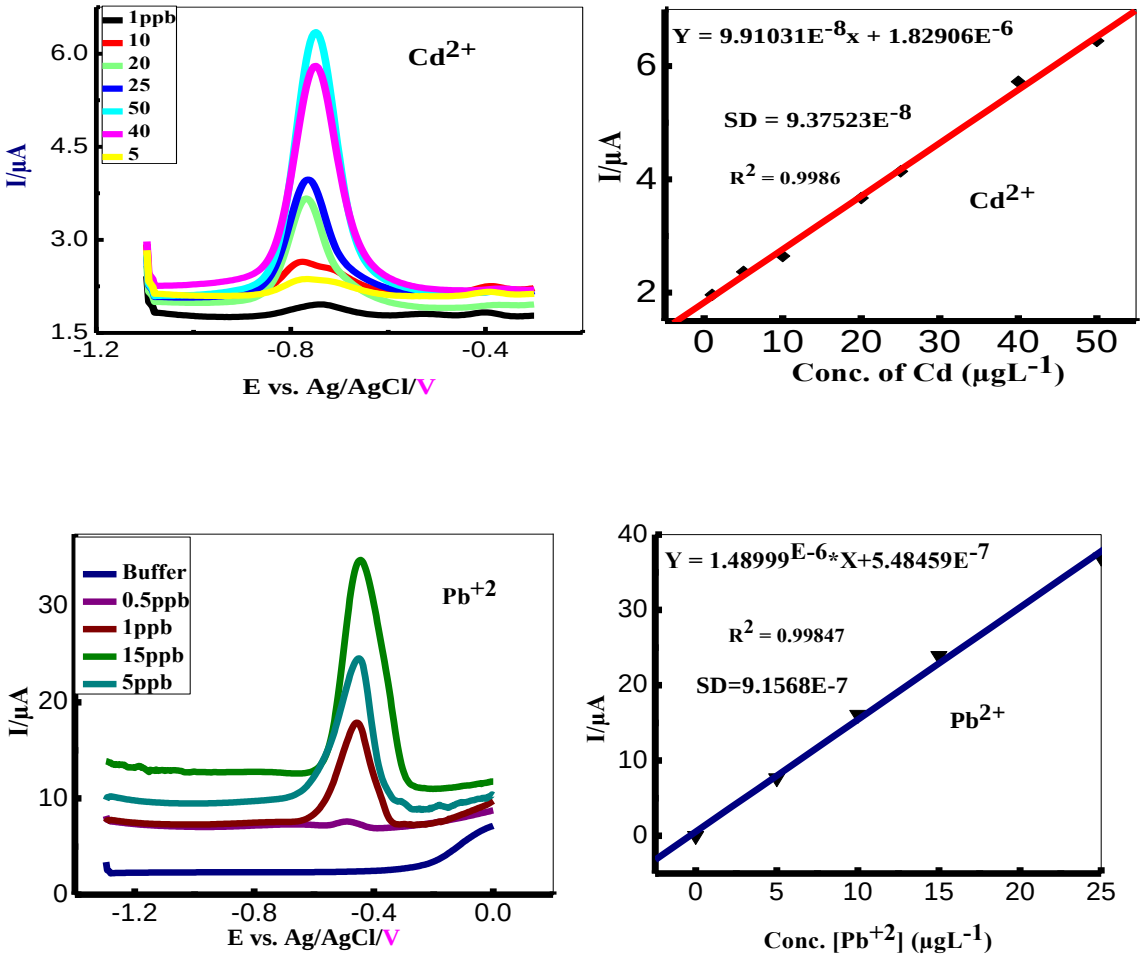

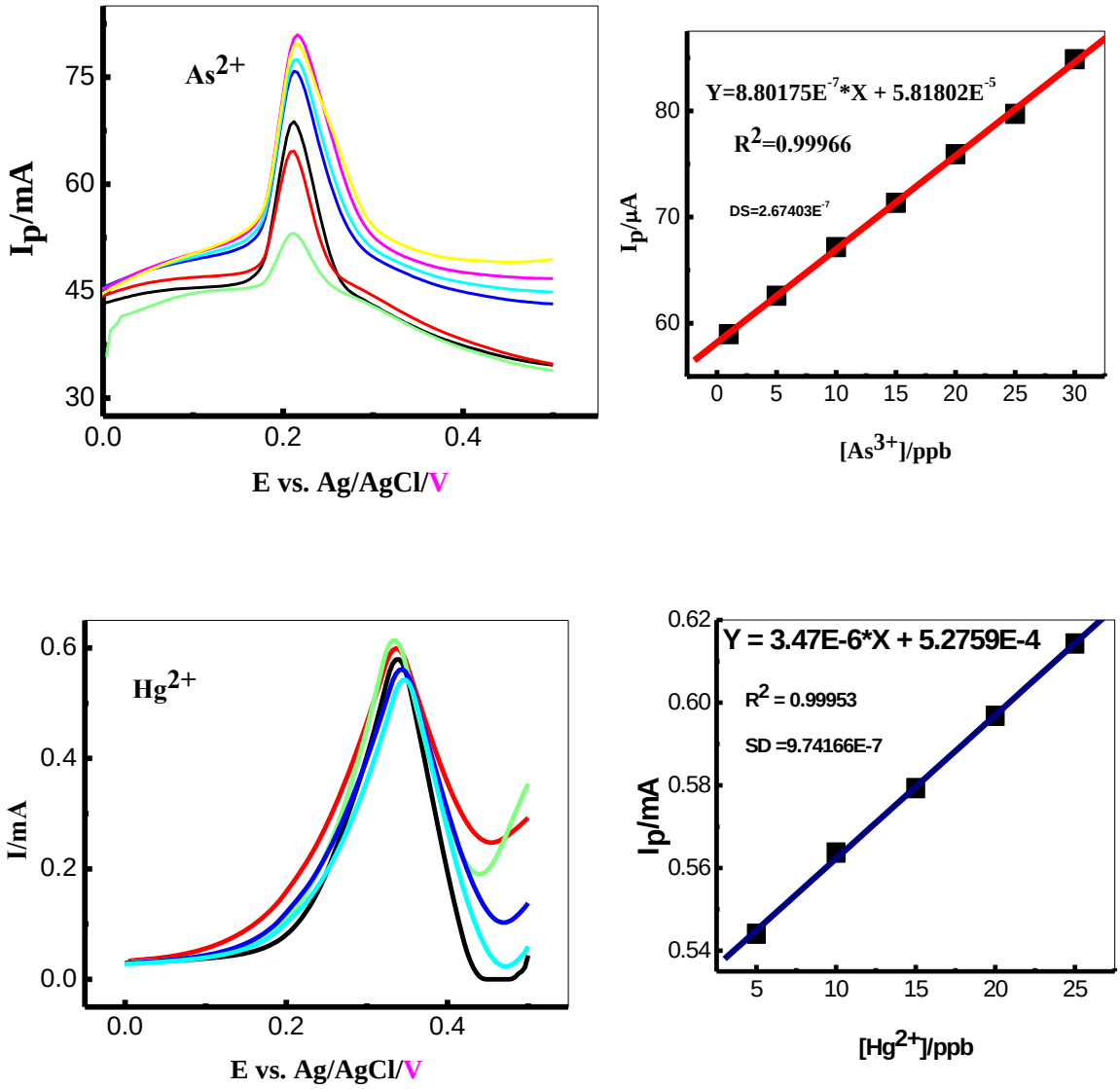

Figure20. OSW-ASV Voltammograms of Cd^{2+}, Pb^{2+}, As^{3+} and Hg^{2+}at d/t conc and at pH 5.2 NaA buffer, deposition time 90 sec and scan rate of 60 mVs^{-1} and its Calibration curve plot of current verse conc. of [Cd^{2+}, Pb^{2+}, As^{3+} and Hg^{2+}]ppb, respectively.

Figure 20 shows the the calibration curves of current verse concentrations of standred solution of Cd, Pb, As and Hg under the optimum experimental conditions within the linear range from 5.0 to 25.0 ppb a characteristic peak was detected at a potential of (-0.7, -0.45, +0.21 and +0.33)V, respectively. A lower limit of detections (LOD) are calculated by use of the formula LOD=3δ/m (where 'δ' is the standard deviation of the plot and 'm' is the slope of

thecalibration plot)to be of 2.8, 1.84, 0.21 and 0.84 ppb for Cd, Pb, As and Hg metals, respectively. From calibration curve plot the sensitivity of modified electrode was determined by using the slope of calibration plot (m) was 0.0937, 1.4, 0.88 and 3.47 and the standard deviation (δ) was 0.099, 0.092, 0.27 and 0.974 0, respectively.

4.9. Determination of THM in Real Samplesby Using PANI-ZnO/GCE

The OSW-ASV of Cd^{2+}, Pb^{2+}, As^{3+} and Hg^{2+} were shown in Fig 20. At optimized parametersthe concentration of Cd^{2+}, Pb^{2+}, As^{3+} and Hg^{2+} was estimated from the calibration curves.From the calibration curves plotted for the known standard solution of Cd, Pb, As and Hg, the unknown concentration of Cd, Pb, As and Hg(value of X) was successfully calculated by using equation y = B*x + A obtained from the calibration curves of the standard solution (where "B" isslope and "A" isintercept were obtained from the calibration carves of each standard solutions of the metal and the value of and "Y" is peak current obtained from the OSW-ASVvoltammogram) (Appendix table 4).

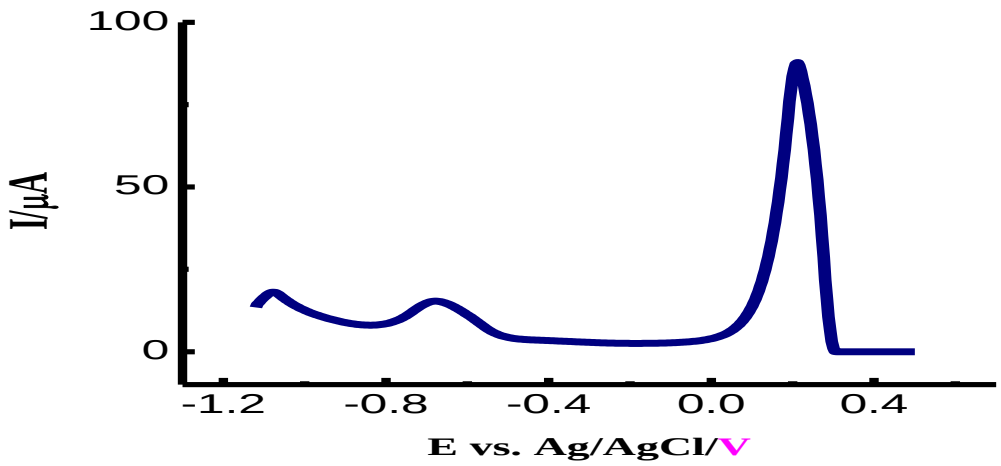

Figure 21. OSW-ASV Voltammograms for GW samples at optimum experimental condition

Figure 21 shows the presence of some metal in a real sample collected from Medigha Woreda, Eastern Harareghe Zone, Oromiya Reginal State, Ethiopia. The metal which are found in that potential detected ions are As and Cd whose concentration in the sample are 20.1 and 4 ppb, respectively. The concenteration of Arsenic in the real sample is higher than the maximum permissible levels of WHO (5, 5, 10 and 5) ppb for (Cd, Pb, As& Hg) ions in water, respectively.

4.10. Co-detection of Cd, Pb, As and Hg Metal Using PANI-ZnO/GCE

OSW-ASV methods alternative promising technique and recommended for simultaneous determination of toxic heavy metals concentration in waste water. In this work, by fixing all the most appropriate conditions, the amount of Zn, Cd, Pb, As and Hg were measured simultaneously in standard solution then water sample after depositing and reducing each metal ion to their specific potentials one after the other. As can be seen from Figure 22, the experimental result obtained by this method do not show totally the oxidation peak current for Hg and the amount of Cd, Pb, and As calculated was also not satisfactory as in case of individual determination and this might be due to the formation of inter metallic and deposition of other metals while depositing one metal.

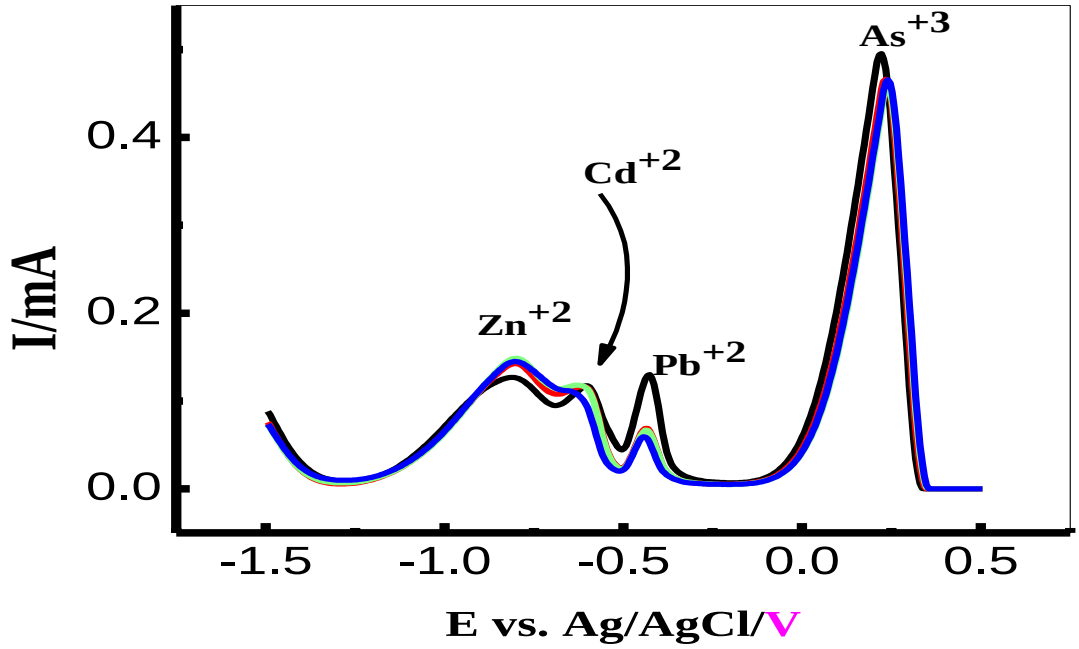

Figure 22. Simultaneous SWASV response of Zn, Cd, Pb and As at concentration of 5, 10, 25 and 50 µg/l, pH 5.2 NaAC buffer, deposition time 90 sec.

5. SUMMARY, CONCLUSIONAND RECOMMENDATIONS

5.1. Summary and Conclusion

Voltammetric techniques are an attractive and suitable electrochemical method for detection of trace level of toxic heavy metals concentration in water samples. The proposed method based on OSW-ASV analysis provides an advantageous over other analytical methods because of its rapid, low cost of equipment, maintenance, higher sensitivity, lower operational cost as it only uses nitrogen or argon gas for purging and without any requirement for cooling of the system, pre concentration is performed directly in the voltammetric cell. However, sample preparation played an important role in ensuring the accuracy of determination because trace metals were often present in low concentrations.

ZnO, PANI and PANI/ZnO nanocomposite were synthesized chemically by *precipitation and in−situ oxidation polymerization method*, respectively and characterized by Uv−vis, FT−IRsp ectra, HR−SEM and HR−TEM image. On other hand PANI and APANI/ZnO synthesized ele ctrochemically by electropolymerization method on GCE using CV. Both chemically and electrochemically as synthesized nanocomposite were characterized by cyclic voltammetry in 1.0 M HCl aqueous solution. The cyclicvoltammetry shows that the deposited PANI on ZnO/GCE was more electroactive this is due to high surface area and catalytic effect ofZnO.

In this work, PANI modified ZnO/GC electrode was used successfully as an electrochemical sensor for the detection of Cd(II), Pb(II), As(III) and Hg(II) individually and simultaneously with very low detection limits. The merits of polymer-modified electrode are: enhanced electro analytical sensitivity, stability and increased mass transport that facilitate estimation of heavy metals at trace levels. Thus, the PANi-ZnO/GCE modified electrode can be a suitable candidate for the detection of heavy metals. Further optimization using this polymer modified electrode to detect nanomolar/sub-nanomolar level of heavy metals and also the simultaneously detection of other heavy metals without involving the pre-concentration step is in progress.

The developed method is based on the enhanced peak current response of toxic heavy metals reduction at PANI-ZnO modified electrode. Compared to the poor response at bare glassy

carbon electrode and PANi/GCE the reduction at the modified electrode was greatly improved. Because of the very rich electrochemical properties of PANI-ZnO, they act as electron mediators thus operating as electron relays for activation of reduction of the analyte. This novel sensing system for heavy metals was convenient and showed excellent analytical characteristics such as significant lowering of the detection limit, high sensitivity and satisfactory selectivity.

5.1. Recommendations

The fabricated nanostructured PANI-ZnO/GCE working electrode could be tried for the determination of very low concentration of toxic heavy metals in various environmental samples like soil, plant, food and medicine.

6. REFERENCES

Alam, M. Alandis, N. M., Ansari, A. A. and Shaik, M. R. 2013. Optical and electrical studies of polyaniline/ZnO nanocomposite. *Journal of Nanomaterials,* 1:1-5.

Aldridge, W. N. 1950. Some properties of specific choline-sterase with particular reference to the mechanism of inhibition by diethyl p-Nitrophenyl Thiophosphate(E605) and analogies. *Biochemical Journal*, 46(4):451-460.

Alimujiang, F. 2010. Mechanical Characterization and Electrochemical Sensor applications of Zinc, Printed by LiU-Tryck, Linköping, Sweden.

Ameen, S., Akhtar, M. S., Ansari, S. G., Yang, O. and Shin, H. S. 2009. Electrophoretically deposted polyaniline/ZnO nanoparticles for p−n heterostructure diodes. *Superlattices and Microstructures*, 46: 872–880.

Arjomandi, J. and Tadayy Arjomandi, J. and Tadayyonfar, S. 2013. Electrochemical synthesis and in situ Spectroelectrochemistry of conducting polymer nanocomposites. Polyaniline/TiO_2, Polyaniline/ZnO, and Polyaniline/TiO_2 + ZnO. *Society of Plastics Engineers*, 253:132-142.

ASHE, W. F., LARGENT, E. J., DUTRA, F. R., HUBBARD, D. M. and BLACKSTONE, M. 1953. Behavior of mercury in the animal organism following inhalation. *Electrochemistry Communications,*7(1):19-43.

Babu, K. S. and Narayanan, V. 2013. Hydrothermal Synthesis of Hydrated Zinc Oxide Nanoparticles and its Characterization. *Chemical Science Transactions,* 2(S1), S33-S36.

Balasubramanian, K. and Burghard, M. 2006. Biosensors based on carbon nanotubes. Analytical and Bioanalaytical Chemistry, 385:452-468.

Ballav, N. and Biswas. M. 2003. Preparation and evaluation of nanocomposites of polythioph ene with Al_2O_3. *Polymer International Journal*, 52: 179-184.

Bard, A.J. and Faulkner, R. L. 2001. "Electrochemical Methods Fundamentals And Applications" John Wiley & Sons, Inc, New York pp. 580-631.

Bard, J., Inzelt G. and Scholz, F. 2008. Electrochemical Dictionary, Verlag Berlin Heidelberg, Germany: Springer.

Bashami, R. M., Hameed, A., Ismailab, M. I. and Soomro, M. T. 2015. The Suitability of ZnO Film Coated Glassy Carbon Electrode for the Sensitive Detection of 4-Nitrophenol in Aqueous Medium. *Analytical methods*, 7:1794–1801.

Buffle, J. and Tercier, W.L. 2009. Analysis of dissolved metal fractions in coastal waters. An inter-comparison of five voltammetric in situprofiling systems. *Journal of Marine Chemistry*, 114: 47-55.

Chen, S.S., Wen, T. C. and Gopalan, A. 2003. Electro synthesis and characterization of a conducting copolymer having S–S links. *Synthetic Metals*, 132: 133–143.

Chen, L., Su, Z., He, X., Liu, Y., Qin, C. Zhou, Y., Li, Z., Wang, L., Xie, Q. and Yao, S. 2012. Square wave anodic stripping voltammetric determination of Cd and Pb ions at a Bi/Nafion/thiolated/polyaniline/glassy carbon electrode. *Electrochemistry of Communication*. 15:34-37.

Deng, J., He, C.L., Peng, Y., Wang, J., Long, X., Li, P. and Chan, A. C. 2003. Magnetic and conductive Fe_3O_4/Polyaniline nanoparticles with core shell structure. *Synthetic Metals*, 139: 295–301.

Deshpande, N.G., Gudage, Y.G., Sharma, R., Vyas, J.C., Kim, J.B. and Lee, Y.P. 2009. Studies on tinoxide intercalated polyaniline nanocomposites for ammonia gas sensing applications. *Sensors and Actuators B: Chemical,* 138: 76–84.

Dhara, S. (2007). "Formation, Dynamics, and Characterization of Nanostructures by Ion Beam Irradiation".*Critical Reviews in Solid State and Materials Sciences*.32(1): 1–50.

Diamond, D. 1998. Principles of Chemical and Biological Sensors. New York: John Wiley So ns.

Durkalec, M., Szkoda, J., Kolacz, R., Opalinski, S., Nawrocka, A. and Zmudzki, J. 2015. Bioaccumulation of lead, cadmium and mercury in roader and wild boars from areas with different levels of toxic metal pollution. *International Journal of Environmental Resource, 9*: 205–212.

Ebrahim, S., El Raey, R., Hefnawy, A., Ibrahim, H., Soliman, M. and Abdel Fatah, T.M. 2013. Electrochemical sensor based on polyaniline nanofibers/single wall carbon nanotubes composite for detection of malathion**.***Synthetic Metals,* 190: 13-19.

Ehi-Eromosele, C. and Okiei W. O. 2012. Resources and Environment management. *Energy and Environmental Science*, 2(3):82-86

Evans, E. H., Day, J. A., Palmer, C. D., Price, W. J., Smith, C. M. M. and Tyson, J. F. 2005. Atomic Spectrometry update. Advances in atomic emission, absorption, and fluorescen ce spectrometry, and related techniques. *Journal of Analytical Atomic Spectrometry*, 20: 562–590.

Genies, E. M. and Tsintavis, C. 2002**.** Redox mechanism and electrochemical behavior or polyaniline deposits. *Journal of Electroanalytical Chemistry and Interfacial Electrochemistry,*195: 109-128.

Goyer, R.A. and Myron, A. M. 1997.Study of heavy metals in the soils. Academic press, New York. 86-89.

Granstroem, M., Magnus, B., Danilo, P., Olle, I.R., Thomas, H. and Olof, W. 1997. Self Organizing Polymer film a route to novel electronic devices based on conjugated polymers. *Super a molecular Science,* 4: 27-34.

Greenhalgh, R., Baron, R. L., Desmoras, J., Engst, R., Esser, H. O. and Klein, W. 1980. Definition of persistence in pesticide chemistry. *Journal of Pure and Applied Chemistry,* 52: 2563-2566.

Grzeszczuk, M. and Szostak, R. 2003. Electrochemical and Raman studies on the redox switch ing hysteresis of polyaniline. *Solid State Ionics,* 157: 257–262.

Gurunathan, K., Amalnerkar, D.P. and Trivedi, D.C. 2003. Synthesis and characterization of conducting polymer composite (Pani/TiO_2) for cathode material in rechargeable battery. *Materials Letters,* 57: 1642–1648.

He, X., Su, Z., Xie, Q., Chen, C., Fu, Y., Chen, L., Liu, Y., Ma, M., Deng, L., Qin. D., Luo, Y. and Yao, S. 2011. Differential pulse anodic stripping voltammetric determination of Cd and Pb at a bismuth glassy carbon electrode modified with Nafion, poly(2,5-dimercapto-1,3,4-thiadiazole) and multiwalled carbon nanotubes. *Microchim Acta*, 173: 95–102.

Hughes, M. F., Beck, B. D., Chen, Y., Lewis, A. S. and D. J. Thomas. 2011. Arsenic exposure and toxicology: a historical perspective. *Toxicological Science*, 123:305–332,

Gerard, M., Chaubey, A., and Malhotra, B. D. 2002.Application of conducting polymers to biosensors.*Biosensors and Bioelectronics*, 17:345–359.

Inzelt, A. 1994.Restructuring of the Hungarian manufacturing industry. *Technology in Society,* 16(1): 35-63.

Inzelt, G., Pineri, M., Schultze, J.W. and Vorotyntsev, M.A. 2000. Electrons and protons in conducting polymers: recent developments and prospects. *Electrochemical Acta,* 45: 2403-2421.

Iwuoha, E.I. and Smyth, M.R. 2003.Reactivities of organic phase biosensors: Square-wave and differential pulse studies of genetically engineered cytochrome P450cam (CYP101) bio-electrodes in selected solvents. *Biosensors and Bioelectronics,*18: 237-244.

Jang, Je-Hun., Brian, A., Dempsey, William, D. and Burgos. 2008. Reduction of U (VI) by Fe (II) in the presence of hydrous ferric oxide and hematite: Effects of solid transformation, surface coverage, and humic acid. *Water Research,* 42: 2269-2277.

Jia, W., Segal, E., Kornemandel, D., Lamhot, Y., Narkis, M. and Siegmann, A. 2002. Polyanilines DBSA/organophilic clay nanocomposites: synthesis and characterization. *Synthetic Metals,* 128: 115–120.

Johnson, R. 2011. Journal of Materials Chemistry Article on graphene oxide–hydrogel networks highlighted by ACS. *Journal of Materials Chemistry Blog,* 21:3534–3550

Juanjuan, M., Xiaobo, Z., Chong, Y., Tong, Z. and Inoue, H. 2008. Synthesis and characterization of a polyaniline/$HTiNbO_5$ lamellar hybrid nanocomposite. *Journal of Mater and Science,* 43:5534–5539.

Kaur B. R. Srivastava, B. Satpati, 2015. Ultra trace detection of toxic heavy metal ions found in water bodies using hydroxyapatite supported nanocrystalline ZSM-5 modified electrodes.*NewJournal Chemistry*.39: 5137–5149.

Kim, B.H., Jung, J.H., Hong, S.H., Kim, J.W., Choi, H.J. and Joo, J. 2001. Physical characterization of emulsionintercalated PANi clay nanocomposite, *Current Applied Physics*, 224: 112–115.

Kukla, A.L., Kanjuk, N.I., Starodub, N.F. and Shirshov, Y.M. 1999. Multienzyme electrochemical sensor array for determination of heavy metal ions. *Sensors and Actuators B,* 57: 213-218.

Kuo, C.T. and Chen, C.H. 1999. Characterization of polyaniline doped with diphenylphosphate. *Synthetic Metals,* 99: 163–167.

Lanje, A. S., Sharma, S. J., Ningthoujam, R. S., Ahn, J. S. and Pode, R. B. 2013.Low temperature dielectric studies of zinc oxide (ZnO) nanoparticles prepared by precipitation method. *Advanced Powder Technology*, 24: 331–335.

Laska, J. 2004. Conformations of polyaniline in polymer blends. *Journal of Molecular Structure*, 701: 13–18.

Li, F. and Tan, T.C. 1994. Monitoring BOD in the presence of heavy metal ions using a poly (4-vinylpyr-idine) coated microbial sensor. *Biosensor,* 9:445–455.

Li, J., Feng, H., Feng, Y., Zhang, Y., Jiang, J. and Qian, D. 2015. Fabrication of gold nanoparticles decorated reduced grapheneoxide as a high performance electrochemical sensing plat form for the detection of toxicant Sudan I.

Li, L., Jiang, J. and Xu, F. 2007. Synthesis and ferromagnetic properties of novel Sm substitut ed LiNiferrite–polyaniline nanocomposite. *Materials Letters,* 61: 1091–1096.

Liu, Y., Feng, X., Shen, J., Zhu, J. J. and Hou. W. 2008. Fabrication of a Novel Glucose Biosensor Based on a Highly Electroactive Polystyrene/Polyaniline/Au Nanocomposite. *Journal of physical chemistry B, 112:* 9237–9242.

Mahmoudian, M.R., Alias, Y., Basirun, W.J., Woi, P.M., Sookhakian, M. and Sheini, J. 2015. Synthesis and characterization of Fe_3O_4 rose like and spherical/reduced grapheneoxide nanosheet composites for lead (II) sensor. *Synthetic Metals,*169: 126-133

March .V, T.D. Nguyen, B. Piro. 2015. Modified electrodes used for electrochemical detection of metal ions in environmental analysis. Biosensors, 5:241–275.

Mathebe, N.G.R., Morrin, A. and Iwuoha, E.I. 2004. Electrochemistry and scanning electron Microscopy of polyaniline/peroxidase based biosensor.Talanta, 64: 115 20. Absorption spectrometry. *Talanta,* 137: 148–155.

Mo, T.C., Wang, H.W., Chen, S.Y. and Yeh, Y.C. 2008. Synthesis and dielectric properties of Polyaniline/titanium dioxide nanocomposites. *Journal of Ceramics International*, 34:1 767–1771.

Monk, P. 2001. Fundamental of Electroanalytical Chemistry: JohWiley & Sons. Chichester, Chichester, Ltd.

Montes-Bayon, M., DeNicola, K. and Caruso, J.A. 2003. Liquid chromatography-inductively coupled plasma mass spectrometry. *Journal Chromatography A, 1000*: 457–476.

Morrin, A., Moutloali, R.M., Killard, A.J., Smyth, M.R., Darkwa, J. and Iwuoha, E. I. 2004. Electrocatalytic sensor devices: (I) cyclopentadienylnickel(II) thiolato Schiff base monolayer self-assembled on gold. *Talanta*, 64:30–38.

Morrin, A. 2002. Characterisation and optimisation of an amperometric biosensor for use in electrochemical immunosensing. Report for Transfer to PhD Register. Dublin City University, Ireland.

Mostafaei, A. and Zolriasatein, A. 2012. Synthesis and characterization of conducting polyane lin nanocomposites containing ZnO nanorods. *Journal of Progress in Natural Science: Materials International,* 22(4): 273–280.

Murray, R. W. 1992. "Molecular Design of Electrode Surfaces," Vol. XXII in the series, Techniques in Chemistry," A. Weissberger, Founding Ed., Wiley-Interscience, New York

Navas-Acien, A., Guallar, E., Silbergeld, E. K. and Rothenberg, S. J. 2007. Lead exposure and cardiovascular disease-A systematic review. *Environmental Health Perspectives*, 115:472-482.

Olad, A., Barati, M. and Shirmohammadi, H. 2011. Conductivity and anticorrosion performance of polyaniline/zinc composites: investigation of zinc particle size anddistribution effect. *Progress in Organic Coatings,* 72: 599–604.

Patil, R.C. and Radhakrishnan, S. 2006. Conducting polymer based hybrid nanocomposites for enhanced corrosion protective coatings. *Progress inorganic Coatings,* 57: 332–336.

Peng, C., Zhang, S., Jewell, D. and Chen, G.Z. 2008. Carbon nanotube and conducting polymer composites for super capacitors. *Progress In Natural Science,* 18: 777–788.

Prabu, P. C. 2009. Impact of heavy metal contamination of akaki river of Ethiopia on soil and metal toxicity on cultivated vegetable crops. *Electronic Journal of Environmental, Agricultural and Food Chemistry,* 8:818-827.

Prasad, G.K., Takei, T., Yonesaki, Y., Kumada, N. and Kinomura, N. 2006. Hybrid nanocomp osite based on $NbWO_6$ nanosheets and polyaniline. *Materials Letters,* 60: 3727–3730.

Pron, A. and Rannou, P. 2001. Process able conjugated polymers: from organic Semi conductors to organic metals and superconductors. *Journal of Progress in Polymer Science,* 27 : 135-190.

Pruneanu, S., Veress, E., Marian, I. and Oniciu, L. 1999. Characterization of polyaniline by cy clicvoltammetry and UV-Vis absorption spectroscopy. *Journal of Materials Science*, 34**:** 2733–2739.

Pud, A., Ogurtsov, N., Korzhenko, A. and Shapoval, G. 2003. Some aspects of preparation methods and properties of polyaniline blends and composites with organic polymers. *Journal of Progress in Polymer Science*, 28: 1701-1753.

Saha, S. and Dollery, C. 2006. Severeis chaemic cardiomyopathy associated with chat chewing. *Journal of the Royal Society of Medicine,* 99:316–318.

Sakthivel, S., Shekar, B.C.,Mangalaraj,D., Narayandass, B.S.K., Venkatachalamb, S. and Prabhakaran, P.V. 1997. Structure, Dielectric, AC and DC Conduction Prpoerties of acidDoped Polyaniline Films.*European Polymer Journal,* 33: 1747-1752.

Satarug, S., Garrett, S. H., Sens, M. A. and Senns, D. A. (2011). Cadmium environmental exposure and health outcomes. *Environmental HealthPerspectives,* 118:182-190.

Sathiyanarayanan, S., Azim, S.S. and Venkatachari, G. 2007. Preparation of polyaniline–TiO_2 composite and its comparative corrosion protection performance with polyaniline. *Synthetic Metals,* 157: 204–205.

Sathiyanarayanan, S., Karpakam, K., Muthukrishnan, S. and Venkatachari, G. 2010. Sulphonate doped polyaniline containing coatings for corrosion protection of iron. *Surface and Coatings Technology,* 204: 1426–1431.

Sharma, P. and Dubey, R. S. 2005.Lead toxicity in plants. *Brazilian Journal of Plant physiology*, 17:35-52.

Sharma, S.K., Sehgal, N. and Kumar, A. 2003. Biomolecules for development of biosensors and their applications. *Current Applied Physics*, 3: 307-316.

Shi, L., Wang, X., Lu, X., Yang, L. and Wu, X. 2009. Preparation of TiO_2/polyaniline nanocomposite from alyotropic liquid crystalline solution. *Synthetic Metals*, 159: 525–2529.

Skoog, A. D., Holler, I. E. and Nieman, A. T. (1998).Principles of instrumental analysis. Harcourt Brace and Co. Ltd, Philadelphia.

Stejskal, J., Sapurina, I. and Trchova, M. 2010. Polyaniline nanostructures and the role of aniline oligomers in their formation. *Progress in Polymer Science*, 35: 1420–1481.

Taillefert, M., Luther, G.W. and Nuzzio, D.B. 2000. The Application of Eletrochemical Tools for in situ Measurements in Aquatic Systems. *Electroanalysis,* 12: 401–412.

Tilahun, E. 2009. Determination of trace metals in commercially available khat (*Cathaedulis-Forsk*) in Addis Ababa.Msc. thesis.Addis Ababa University.33-42.

Tovidea, O., Jaheeda, N., Mohameda, N., Nxusania, E., Sundaya, C. E., Tsegayea, A., Ajayia, R.F. Njomoa, N., Makelanea, H., Bilibanaa, M., Bakera, G., Williamsb, A., Vilakazic, S., Tshikhudoc, R. and Iwuohaa, E. I. 2014. Graphenated polyaniline-doped tungsten oxide nanocomposites sensor for real time determination of phenanthrene. *Electrochimica Acta*, 128: 138–148.

US EPA. 2009. *Drinking Water Contaminants*; United States Environmental Protection Agency (EPA): Washington, DC, USA.

Wang, Z., Liu, E. and Zhao, X. 2011. Glassy carbon electrode modified by conductive polyaliline coating for determination of trace lead and cadmium ions in acetate buffer solution. *Thin Solid Films*, 519: 5285–5289.

Wang, L., Lu, X., Lei, S. and Song, Y. 2000. Graphene oxide-based polyaniline nanocomposites: preparation, properties and applications. *Journal Material Chemistry*, 2:4491-4509.

Wang, J., Musameh, M. and Lin, Y. 2003. Solubilization of carbon nanotubes by nafion toward the preparation of amperometric biosensors. *Journal of American Chemical Society*, 125: 2408-2409.

Wang, B., Chang, Y. L., and Zhi, 2011. New Carbon Materials.*Electrochimica Acta*, 26: 31-40.

Wang, L., Lu, X., Lei, S. and Song, Y. 2014. Graphene based polyaniline nanocomposites: preparation, properties and applications. *Journal of Material Chemistry*, 2: 4491–4509.

Wei, Y., Yang, R., Yu, X., Wang, L., Liu J. and Huang, X. 2012. Stripping voltammetry study of ultra-trace toxic metal ions on highly selectively adsorptive porous magnesium oxide nanoflowers. *Electrochemistry Communications*, 10: 45–49

Wei, Y., Gao, C., Meng, F. L., Li, H. H., Wang, L., Liu, J. H. and Huang, X. J. 2012. SnO_2/Reduced graphene oxide nanocomposite for the simultaneous electrochemical detection of cadmium(II), lead(II), copper(II), and mercury(II): an interesting favorable mutual interference. *Journal of Physical Chemistry*, C 116: 1034-1041.

Wong, L. S., Chow, E. and Gooding, J. J. 2007. The electrochemical detection of cadmium using surface-immobilized DNA.*Electrochemistry Communications*, 9: 845–849.

World Health Organization 2008. Guidelines for drinking water quality.World Health Organization, Geneva.

Xu, J.C., Liu, W.M. and Li, H.L. 2005. Titaniumdioxide doped polyaniline. *Materials Science and Engineering*, 25: 444–447.

Yerawar, G. R. 2012. Characterization of Chemically Synthesized Polyaniline-Zinc Oxide Nanocomposites. *DerPharma Chemica*, 4(3):1288-1291.

Yin, H.S., Zhou, Y. and Ai, S-Y. 2009. Preparation and characteristic of cobalt phthalocyanine modified carbon paste electrode for bisphenol detection.

Zhang, S., Wang, N., Niu, Y. and Sun, C. 2004. Immobilization of glucose oxidase on gold na noparticles modified Au electrode for the construction of biosensor. *Sensors and Actuators B: Chemical*, 109: 367-374.

Zhang, X., Ji, L., Zhang, S. and Yang, W. 2007. Synthesis of a novel polyaniline intercalated Layered manganese oxide nanocomposites as electrode material for electrochemical capacitor. *Journal of Power Sources,* 173: 1017–1023.

Zhang, Y. and Adeloju, S.B. 2015. Coupling of non-selective adsorption with selective elution for novel in-line separation and detection of cadmium by vapor generation atomic absorption spectrometry. *Talanta,* 137: 148–155.

7. APPENDIX

Table 7. Summary of electrochemical parameters evaluated form the CV of 2 Mm $K_3Fe(CN)_6$

Scan rate	$V^{1/2}$	lnV	E_{pa}/ mV	i_{pa}/A	E_{pc} /mV	i_{pc}/A	i_{pa}/i_{pc}	ΔEp/mV	$E^{0'}$/mV
10	3.2	2.3	248.1	$1.176e^{-5}$	184.1	$-1.802\ e^{-5}$	0.7	64.0	217.05
25	5.0	3.2	254.2	$2.074\ e^{-5}$	179.1	$-2.553\ e^{-5}$	0.8	75.1	216.70
50	7.1	3.9	258.6	$3.043\ e^{-5}$	174.2	$-3.362\ e^{-5}$	0.9	84.4	216.05
75	7.7	4.3	261.1	$3.537e^{-5}$	172.5	$-3.537\ e^{-5}$	1.0	88.6	216.05
100	10.0	4.6	262.2	$4.335\ e^{-5}$	170.5	$-4.415\ e^{-5}$	1.0	93.5	215.45
150	12.2	5.0	264.7	$5.266\ e^{-5}$	168.0	$-5.226\ e^{-5}$	1.0	97.3	216.05
200	14.1	5.3	266.9	$6.144e^{-5}$	167.3	$-5.894\ e^{-5}$	1.1	99.6	217.10

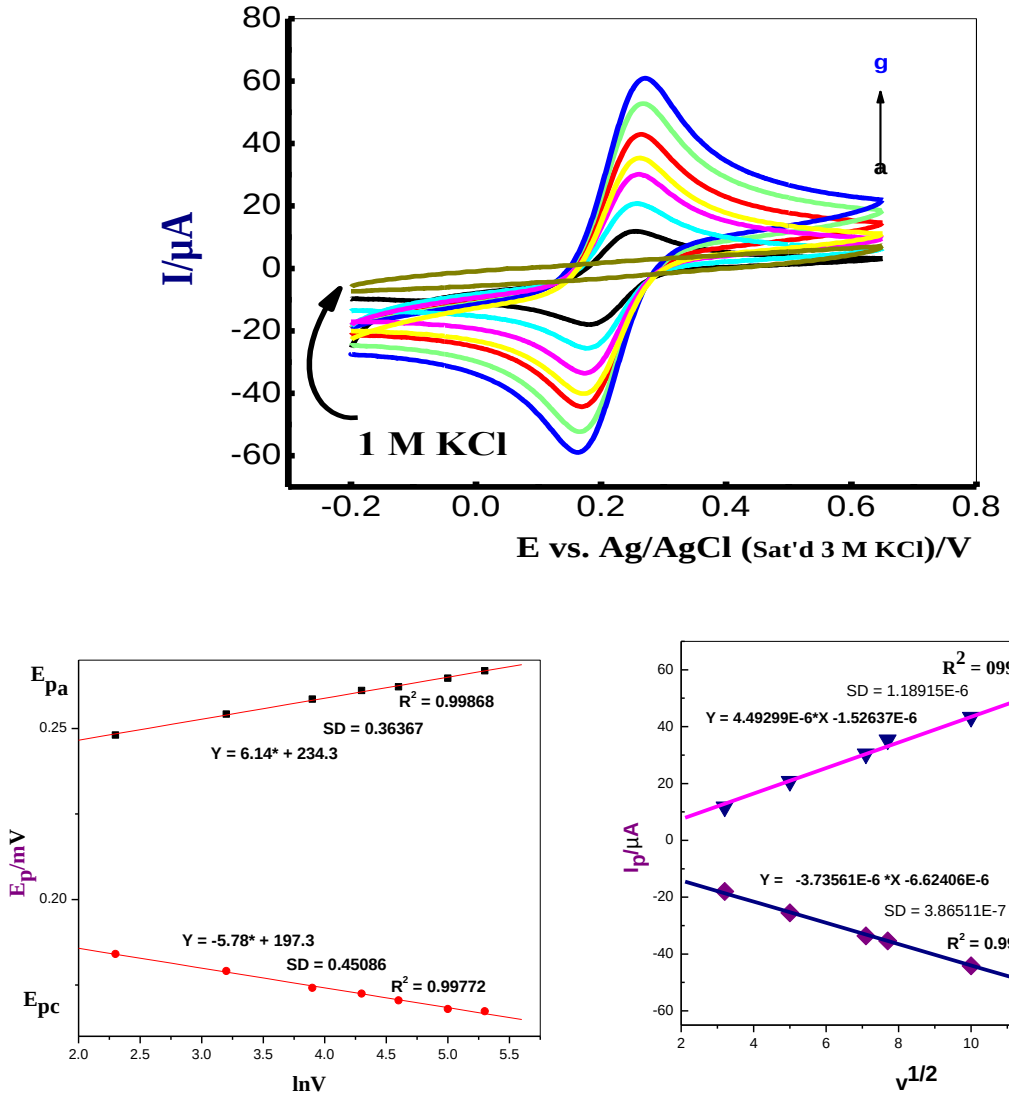

Figure 23. CV of GCE of 2 Mm of $K_3[Fe(CN)_6]$/1.0 M KCl: potential window 0.2 to + 0.65V; at different scan rates (10, 25, 50, 75, 100, 150, 200) mVs^{-1}.The inset plot shows the plot of the scan rate dependence of its Ip vs. $V^{1/2}$ and E_P vs. lnV

Table 8. Electrochemical characterization parameters of PANI/ GCE

PANI /GCE	ν	Oxidation/Reduction AA'				Oxidation/Reduction BB'				Oxidation/Reduction CC'			
		$E_{pa,}$ mV	I_{pa} (mA)	$E_{pc,}$ mV	I_{pc} (mA)	$E_{pa,}$ mV	I_{pa} (mA)	$E_{pc,}$ mV	I_{pc} (mA)	$E_{pa,}$ mV	I_{pa} (mA)	$E_{pc,}$ mV	I_{pc} (mA)
5 cycles	5	155.3	3.91e-7	70.8	8.81e-6	424.2	2.71e-7	490.8	1.00e-5	785.2	1.96e-6	744.2	5.74e-6
	10	214.1	4.51e-6	104.1	1.04e-5	539.4	5.50e-6	521.5	1.36e-5	728.9	4.97e-6	631.6	1.52e-5
	25	227.1	1.62e-5	147.7	2.08e-5	539.4	1.69e-5	478.0	2.77e-5	687.9	1.16e-5	598.3	5.75e-5
	50	234.7	3.82e-5	129.7	3.11e-5	536.8	4.03e-5	570.1	1.17e-4				
	75	245.1	6.37e-5	137.4	4.00e-5	547.1	6.50e-5	557.3	1.68e-4				
	100	252.6	8.81e-5	140.1	4.81e-5	542.1	8.81e-5	549.6	2.16e-4				
10 cycles	5	196.1	9.29e-5	60.5	4.42e-5	508.1	1.95e-5	505.6	3.46e-5	769.4	5.85e-5	684.7	5.34e-5
	10	229.8	2.44e-4	75.1	7.38e-5	529.8	6.03e-5	520.2	7.04e-4	740.3	7.98e-5	643.5	1.32e-4
	25	263.7	6.11e-4	91.9	1.53e-4	551.6	1.77e-4	469.4	1.56e-4	706.5	1.50e-4	602.4	3.83e-4
	50	295.2	1.11e-3	116.1	2.77e-4	556.5	3.65e-4	571.1	7.45e-4				
	75	321.8	1.53e-3	125.8	3.85e-4	561.3	5.61e-4	556.5	1.04e-3				
	100	333.9	1.89e-3	128.2	5.05e-4	568.5	7.16e-4	539.5	1.32e-3				
15 cycles	5	226.5	2.75E-4	101.6	-3.31E-5	527.4	-4.06E-5	471.8	2.0E-4	740.3	8.78e-5	602.4	1.81e-4
	10	255.9	6.92E-4	82.3	-1.79E-4	496.1	1.07E-4	469.4	-1.31E-4	757.3	2.06e-4	633.9	4.85e-4
	25	293.8	0.00162	91.9	-4.39E-4	534.7	4.68E-4	471.8	-0.00102	713.7	3.67e-4	592.7	1.21e-3
	50	322.7	0.00263	106.5	-7.55E-4	585.5	8.51E-4	558.9	-0.00202				
	75	339.7	0.00304	123.4	-8.41E-4	580.6	9.7E-4	537.1	-0.0023				
	100	350.1	0.00406	118.5	-0.00119	590.3	0.00139	517.7	-0.00323				

Table 9. Electrochemical parameters of PANI/ZnO/GCE

PANI-ZnO/GCE	*v*	Oxidation/Reduction AA'				Oxidation/Reduction BB'				Oxidation/Reduction CC'			
		$E_{pa,}$ mV	I_{pa} (mA)	$E_{pc,}$ mV	I_{pc} (mA)	$E_{pa,}$ mV	I_{pa} (mA)	$E_{pc,}$ mV	I_{pc} (mA)	$E_{pa,}$ mV	I_{pa} (mA)	$E_{pc,}$ mV	I_{pc} (mA)
5 cycles	5	214.2	4.89e-5	86.2	2.58e-5	544.5	1.92e-5	452.3	2.95e-5	734.0	1.99e-5	613.7	4.87e-5
	10	237.3	1.13e-4	109.2	4.47e-5	544.5	5.03e-5	460.0	4.87e-5	695.6	3.51e-5	575.2	1.33e-4
	25	291.0	3.01e-4	255.2	3.32e-4	554.8	1.28e-4	518.9	3.47e-4				
	50	329.4	4.95e-4	186.1	1.32e-4	552.2	2.03e-4	490.8	5.19e-4				
	75	352.5	9.04e-4	188.6	2.18e-4	559.9	3.78e-4	467.7	9.10e-4				
	100	357.9	1.08e-3	196.3	2.79e-4	562.4	4.92e-4	452.3	1.15e-3				
10 cycles	5	234.7	4.46e-4	175.8	2.34e-4	529.2	8.13e-5	542.0	1.02e-4	757.0	1.17e-4	649.5	1.61e-4
	10	262.9	8.40e-4	101.6	1.57e-4	547.6	1.98e-4	478.1	1.69e-4	721.2	1.71e-4	618.8	3.73e-4
	25	306.4	1.59e-3	147.7	3.38e-3	565.1	5.23e-4	565.1	9.45e-4				
	50	338.7	2.19e-3	155.7	4.86e-4	573.9	8.19e-4	531.9	1.45e-3				
	75	373.1	3.13e-3	180.9	8.08e-4	575.2	1.41e-3	488.2	2.45e-3				
	100	393.5	4.07e-3	178.4	1.06e-3	577.8	1.83e-3	470.3	3.16e-3				
15 cycles	5	230.6	8.82e-4	68.3	-6.01e-5	529.2	1.85E-5	470.3	-1.54e-4	736.6	3.26e-4	606.1	9.37e-4
	10	270.8	1.84e-3	91.3	-4.04e-4	539.4	4.89E-4	465.1	-1.09e-3	716.1	4.79e-4	565.1	1.83e-3
	25	316.6	4.2e-3	129.7	-1.11e-3	572.7	0.00161	516.4	-3.31e-3				
	50	360.6	6.62e-3	127.2	-2.0e-3	577.8	0.00291	483.1	-5.86e-3				
	75	380.7	0.0075	114.4	-2.3e-3	950.6	0.0033	480.5	-6.87e-3				
	100	398.6	9.91e-3	96.4	-3.31e-3	603.4	0.00475	460.1	-9.75e-3				

Table 10. The results obtained for the unknown concentration of metal ions in real sample

Metal ions	Concentration of toxic heavy metals in water samples (mg/L)	
	I_p (μA) obtained from water samples	[THMI]/ppb in water samples
As	75.72	20.1
Cd	0.68	5.0